

## Review

# A review on composite strategy of MOF derivatives for improving electromagnetic wave absorption

Jingpeng Lin,<sup>1</sup> Qilei Wu,<sup>2</sup> Jing Qiao,<sup>1</sup> Sinan Zheng,<sup>1</sup> Wei Liu,<sup>3,4</sup> Lili Wu,<sup>1</sup> Jiurong Liu,<sup>1,\*</sup> and Zihui Zeng<sup>1,5,\*</sup>

## SUMMARY

To address the electromagnetic wave (EMW) pollution issues caused by the development of electronics and wireless communication technology, it is urgent to develop efficient EMW-absorbing materials. With controllable composition, diverse structure, high porosity, and large specific surface area, metal-organic framework (MOF) derivatives have sparked the infinite passion and creativity of researchers in the electromagnetic field. Against the challenges of poor inherent impedance matching and insufficient attenuation capability of pure MOF derivative, designing and developing MOF derivative-based composites by compounding MOF with other materials, such as graphene, CNTs, MXene, and so on, has been an effective strategy for constructing high-efficiency EMW absorbing materials. This review systematically expounds the research progress of MOF derivative-based composite strategies, and discusses the challenges and opportunities faced by MOF derivatives in the field of EMW absorption. This work can provide some good ideas for researchers to design and prepare high-efficiency MOF-based EMW absorbing materials in applications of next-generation electronics and aerospace.

## INTRODUCTION

With the rapid development of modern technology, electronics or communication technology are employed in all aspects of society, which inevitably causes adverse electromagnetic wave (EMW) radiation or pollution.<sup>1–8</sup> This not only results in significant electromagnetic interference to electronics themselves but also endangers human health.<sup>9–11</sup> To address this issue, EMW absorbing materials that can absorb EMW energy by converting it into heat or other forms of energy are highly desired.<sup>12</sup> The ideal EMW absorbing materials require the characteristics of low matching thickness, light weight, wide effective absorption bandwidth (EAB), and high absorption strength.<sup>13,14</sup> Nevertheless, for traditional EMW absorbing materials such as dielectric or magnetic materials, the challenges such as the narrow EAB and low absorption strength at high frequencies exist, which impedes their practical applications.

In general, EMW absorbing materials can be divided into dielectric loss materials and magnetic loss materials.<sup>15</sup> The former is mainly made of various carbon materials, conductive polymers, and so on,<sup>16</sup> and the latter are mainly composed of various magnetic particles and ferrite materials.<sup>15</sup> EMW absorbing materials with a single loss type usually have poor absorbing performance due to impedance mismatch.<sup>17,18</sup> Such as dielectric materials due to the high conductivity and dielectric constant, the impedance matching is not satisfactory. Researchers have found that the combination of dielectric loss materials and magnetic loss materials is one effective way to improve EMW absorbing performance.<sup>19–21</sup> The traditional combination strategy includes electroless plating,<sup>22,23</sup> such as coating the magnetic particles on carbon fiber, and immersion or solvothermal followed by high-temperature carbonization treatments.<sup>24–26</sup> After immersing carbon precursors in a magnetic metal salt solution followed by the calcination, the carbon precursors are converted into carbon and the metal ions are reduced to magnetic metal particles. However, the dispersion of magnetic particles prepared in such methods is not uniform, and the microstructure and performance cannot be accurately controlled.

Metal-organic frameworks (MOFs) are a type of material with periodic network crystal structure, large specific surface area, high porosity, and some characteristics formed by the self-assembly of excessive metal ions and organic ligands.<sup>27–31</sup> Since the first MOF was synthesized by Yaghi et al. in 1995,<sup>32</sup> MOFs and MOF derivatives have been widely used in catalysis,<sup>33–35</sup> energy storage,<sup>36,37</sup> and separation.<sup>38,39</sup> Since 2015,

<sup>1</sup>Key Laboratory for Liquid-Solid Structural Evolution and Processing of Materials, School of Materials Science and Engineering, Shandong University, Jinan 250061, PR China

<sup>2</sup>Science and Technology on Electromagnetic Compatibility Laboratory, China Ship Development and Design Centre, Wuhan 430064, PR China

<sup>3</sup>Institute of Crystal Materials, State Key Laboratory of Crystal Materials, Shandong University, Jinan 250100, China

<sup>4</sup>Shenzhen Research Institute of Shandong University, Shenzhen 518063, PR China

<sup>5</sup>Suzhou Research Institute of Shandong University, Suzhou 215123, PR China

\*Correspondence:  
[jliu@sdu.edu.cn](mailto:jliu@sdu.edu.cn) (J.L.),  
[zihui.zeng@sdu.edu.cn](mailto:zihui.zeng@sdu.edu.cn) (Z.Z.)

<https://doi.org/10.1016/j.isci.2023.107132>



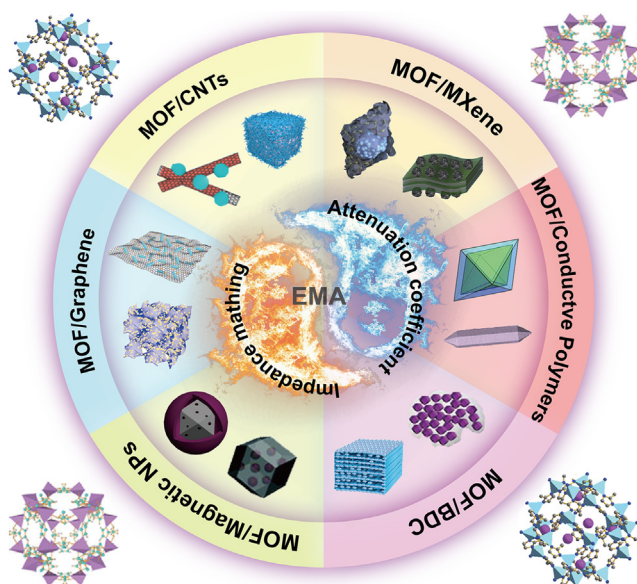


**Figure 1. MOF derivative composites for EMW absorption**

Reprinted and adapted with permission from ref. [47–58](#)

MOF materials have gradually been used in the field of EMW absorption. Lv et al. prepared Co/C nanocomposites for EMW absorption by carbonizing ZIF-67 for the first time.<sup>40</sup> After carbonizing the MOF at 500°C under inert gas, the optimal reflection loss (RL) of Co/C-500 reached  $-35.3$  dB and the EAB was 5.8 GHz. The good EMW absorption properties benefited from the multi-component properties and high porosity which effectively adjusted the impedance matching. Compared with other magnetic carbon materials, the MOF derivatives have some advantages as follows: firstly, due to the periodic framework structure of MOFs, magnetic particles can be uniformly dispersed in a carbon matrix, creating more heterointerfaces while exerting better magnetic effect.<sup>41,42</sup> Secondly, the electrical conductivity of MOF derivatives can be conveniently adjusted by controlling the carbonization temperature.<sup>43</sup> The appropriate conductivity enables the material to have conductivity loss capability with efficient impedance matching. Thirdly, the retained high porosity of MOF derivatives not only facilitates impedance matching but also improves EMW loss capacity through multiple scattering or reflections.<sup>44</sup> Besides, the composition of the MOF derivatives can be changed by controlling the thermal pyrolysis condition. These advantages of MOF derivatives are extremely attractive for the exploration of ideal EMW absorbing materials, and thus numerous reports consider developing the MOF derivatives of EMW absorption materials as one most promising candidates in this field.

However, EMW absorbers prepared from MOF derivatives still suffer from large filling amounts, and narrow EAB due to the severe agglomeration of the MOF derivative particles. Researchers usually employ the strategy of combining MOF derivatives with other components to address the issues. The composites exhibit variable morphology and improved EMW absorption performance. Reviewing the composite strategy of MOF derivatives for preparing EMW absorbing materials is highly desired for understanding the structure-property-method relationships, advancing the development of MOF-based high-performance EMW absorbers. However, rare reports have been devoted to the progress, and a lot of MOF-related review articles focus on the type or structural design of MOF derivatives.<sup>45,46</sup> Herein, the research progress of MOF derivatives combined with other loss materials including graphene, carbon nanotubes (CNTs), transition metal carbides/nitrides (MXenes), biomass-derived carbon (BDC), conductive polymers and magnetic nanoparticles (NPs) for EMW absorbing materials is reviewed (Figure 1). Particularly, the introduction of graphene, CNTs, MXenes, and BDC makes the independent MOF derivatives be efficiently connected. This builds a sufficient network to improve the conductive loss ability of MOF derivatives, promoting the EMW absorbing performance. The performance and EMW loss mechanism of these composites are illustrated by analyzing the typical examples. Finally, the challenges and development directions of MOF-derived composites in the field of EMW absorption are prospected.

## THEORIES OF MICROWAVE ABSORPTION

EMW radiated to the surface of a material has three main destinations. First, a portion of the wave is reflected into free space, called reflected waves. Part of it enters the material and is attenuated by various loss mechanisms under the electromagnetic properties of the material, which is called an absorption wave. The remainder penetrates the material into free space again.<sup>59</sup> An ideal EMW absorber needs to attenuate the EMW as much as possible while generating as few reflected waves as possible.

### Performance evaluation

The EMW absorption performance is determined by electromagnetic parameters, namely complex permittivity ( $\epsilon_r = \epsilon' - j\epsilon''$ ) and complex permeability ( $\mu_r = \mu' - j\mu''$ ). The real part of the complex permittivity and the complex permeability represents the energy storage capacity, and the imaginary part represents the energy attenuation capacity.<sup>60,61</sup> The performance of EMW absorbing materials is evaluated by the RL value, which is calculated by the following equations based on transmission line theory:<sup>62,63</sup>

$$Z_{in} = Z_0 \sqrt{\frac{\mu_r}{\epsilon_r}} \tanh \left( \frac{2\pi j f d}{c} \sqrt{\mu_r \epsilon_r} \right) \quad (\text{Equation 1})$$

$$RL = 20 \log \left| \frac{Z_{in} - Z_0}{Z_{in} + Z_0} \right| \quad (\text{Equation 2})$$

where  $Z_{in}$  and  $Z_0$  are the input impedance of absorber and the impedance of free space, respectively,  $\mu_r$  and  $\epsilon_r$  are the relative complex permittivity and permeability, respectively,  $f$  is the frequency of microwave,  $d$  is the thickness of the absorber, and  $c$  is the velocity of light in vacuum. The smaller the RL value, the stronger the EMW absorption ability. When the RL value is less than  $-10$  dB, it means that 90% of the EMWs are absorbed, and the frequency range of  $RL \leq -10$  dB is defined as an EAB.<sup>64</sup> At present, the research on EMW absorbing materials mainly focuses on the frequency range of 2–18 GHz.

### Influence factors

Impedance matching and attenuation coefficient are the most important influence factors on EMW absorbing materials.<sup>21,65</sup> The impedance matching determines whether the EMW can enter the EMW absorbing material, and the attenuation coefficient determines the attenuation ability of the EMW absorbing material. According to the Fresnel theory, when an EMW is irradiated vertically onto the surface of a material from free space, its reflectivity can be described by the following expression:<sup>65</sup>

$$R = \frac{Z_{in} - Z_0}{Z_{in} + Z_0} \quad (\text{Equation 3})$$

It can be seen from the aforementioned equation that to minimize the reflectivity, the value of  $(Z_{in} - Z_0)$  is required to be 0. Namely, the input impedance of the absorber and the impedance of the free space should be equal ( $Z_{in}/Z_0 = 1$ ). However, for a real material, the real and imaginary parts cannot be kept consistent. Therefore, in some calculations, an absolute value of  $|Z_{in}/Z_0| = 1$  is usually introduced to judge the impedance matching of the absorbers.<sup>55</sup> The equation is shown as follows:<sup>66</sup>

$$|Z_{in}/Z_0| = \left| \sqrt{\frac{\mu_r}{\epsilon_r}} \tanh \left[ \frac{2\pi j f d}{c} \sqrt{\mu_r \epsilon_r} \right] \right| \quad (\text{Equation 4})$$

However, due to the introduction of the absolute value, there still exists a situation where the absolute value is equal to 1 even when the values of  $Z_{in}$  and  $Z_0$  are very different.<sup>65</sup> Therefore, some studies introduce the delta function to evaluate impedance matching. The equation is shown as follows:<sup>49,67</sup>

$$|\Delta| = \left| \sinh^2(Kfd) - M \right| \quad (\text{Equation 5})$$

$$K = \frac{4\pi \sqrt{\mu' \epsilon'} \sin \frac{\delta_e + \delta_m}{2}}{c \cos \delta_e \cos \delta_m} \quad (\text{Equation 6})$$

$$M = \frac{4\mu' \cos \delta_e \epsilon' \cos \delta_m}{(\mu' \cos \delta_e - \epsilon' \cos \delta_m)^2 + \left[ \tan \left( \frac{\delta_m}{2} - \frac{\delta_e}{2} \right) \right]^2 (\mu' \cos \delta_e + \epsilon' \cos \delta_m)^2} \quad (\text{Equation 7})$$

where  $\delta\epsilon$  and  $\delta\mu$  refer to the dielectric loss angle and the magnetic loss angle, respectively. The small delta value close to zero indicates a good impedance matching. If  $|\Delta|$  tends to be far from zero, EMW absorption is poor.

The value of the attenuation coefficient can be calculated by the following equation:<sup>47,68,69</sup>

$$\alpha = \frac{\sqrt{2\pi}f}{c} \sqrt{(\mu''\epsilon'' - \mu'\epsilon') + \sqrt{(\mu''\epsilon'' - \mu'\epsilon')^2 + (\mu'\epsilon'' + \mu''\epsilon')^2}} \quad (\text{Equation 8})$$

It can be seen from the equation that the value of the attenuation coefficient increases with the increase of  $\mu''$  and  $\epsilon''$ ; however, too large values of  $\mu''$  and  $\epsilon''$  will cause the impedance mismatch. Therefore, the best EMW absorption performance can only be achieved if the values of  $\mu''$  and  $\epsilon''$  are kept in a suitable range and both the impedance matching and attenuation coefficient requirements are satisfied.<sup>70</sup>

### EMW loss mechanism

The loss mechanism of EMW absorbing materials is mainly divided into two types: dielectric loss and magnetic loss, and their loss capability can be evaluated by the dielectric loss tangent ( $\tan \delta_\epsilon = \epsilon''/\epsilon'$ ) and the magnetic loss tangent ( $\tan \delta_\mu = \mu''/\mu'$ ), respectively.<sup>71</sup> Dielectric loss involves conductive loss and polarization-relaxation loss.<sup>72</sup> Conductive loss means that the holes and electrons in the material will reciprocate in the presence of alternating electric field, and the microcurrent generated will be dissipated in the form of heat energy due to the resistance of the material.<sup>73</sup> For highly conductive materials, the imaginary part of the permittivity can be influenced by the conductivity as follows:<sup>74</sup>

$$\epsilon'' \approx \sigma/2\pi\epsilon_0 f \quad (\text{Equation 9})$$

where  $\epsilon_0$  is the permittivity of the vacuum. Therefore, improving the electrical conductivity of the material benefits the conductive loss of the absorber. But it is worth noting that too high conductivity will cause the skin effect, which leads to impedance mismatch so that more EMWs are reflected on the surface of the EMW absorbing material, which reduces the EMW absorption performance.<sup>75</sup>

Polarization can be divided into dipole polarization, interfacial polarization, ionic polarization, and electronic polarization.<sup>76</sup> However, ionic and electronic polarizations usually occur at higher frequencies (10<sup>3</sup>–10<sup>6</sup> GHz), which are usually not considered as the loss mechanism of microwave absorbing materials. Dipole polarization refers to the periodic rotation and arrangement of polar molecules and polar functional groups in the material under the incident EMW.<sup>10</sup> Compared with the applied periodically changing alternating electric field, these periodic motions of polar units have a certain relaxation when the electric field energy is converted into thermal energy and dissipated. Interfacial polarization refers to the accumulation of charges at the interfaces of different materials or defects.<sup>77</sup> In the presence of an alternating electric field, charges undergo repeated polarization-relaxation processes to attenuate the EMW. According to Debye theory, complex permittivity can be described by the following expression:<sup>78</sup>

$$\epsilon' = \epsilon_\infty + \frac{\epsilon_s - \epsilon_\infty}{1 + \omega^2\tau^2} \quad (\text{Equation 10})$$

$$\epsilon'' = \omega\tau \frac{\epsilon_s - \epsilon_\infty}{1 + \omega^2\tau^2} \quad (\text{Equation 11})$$

where  $\epsilon_\infty$ ,  $\epsilon_s$ , and  $\epsilon_0$  represent the permittivity at the high-frequency limit, static permittivity, and permittivity of vacuum, respectively.  $\omega$  is the angular frequency, and  $\tau$  is the polarization relaxation time. By merging and simplifying the process, the relationship between  $\epsilon'$  and  $\epsilon''$  can be expressed in the following form:<sup>79</sup>

$$\left(\epsilon' - \frac{\epsilon_s + \epsilon_\infty}{2}\right)^2 + (\epsilon'')^2 = \left(\frac{\epsilon_s - \epsilon_\infty}{2}\right)^2 \quad (\text{Equation 12})$$

The graph plots by the relationship between the  $\epsilon'$  and  $\epsilon''$  are usually called the Cole-Cole plot whose radius is  $\frac{\epsilon_s - \epsilon_\infty}{2}$  and center is  $(\frac{\epsilon_s + \epsilon_\infty}{2}, 0)$ . In the Cole-Cole plot, each semicircle represents a polarization-relaxation process.<sup>80</sup>

Magnetic loss can be divided into natural resonance, exchange resonance, eddy current loss, hysteresis, and domain wall resonance.<sup>81</sup> In EMW absorbing materials, since the magnetic field is too weak to induce hysteresis and the domain wall resonance occurs at a lower frequency, the magnetic loss mainly originates

from natural resonance, exchange resonance, and eddy current.<sup>82</sup> Whether magnetic losses are caused only by eddy current loss can be determined by the following equation:<sup>83</sup>

$$C_0 = \mu''(\mu')^{-2}f^{-1} = 2\pi\mu_0\sigma d^2 / 3 \quad (\text{Equation 13})$$

The value of  $C_0$  is a constant that does not change with frequency if eddy current is the only factor contributing to the magnetic loss. On the contrary, magnetic loss exists not only in the form of eddy current but also in other forms of magnetic loss.

The natural resonances result from ferromagnet maximally absorbing the energy of alternating magnetic fields, which are usually regarded as the most important magnetic attenuation mechanism in high frequency. The damping motion of the magnetic moment around the magnetic anisotropy field is the essence of natural resonances. The natural resonance effect can be expressed by the following equations.<sup>65</sup>

$$(\mu_i - 1)f_r = \frac{1}{3\pi}\gamma M_s \quad (\text{Equation 14})$$

$$H_\alpha = \frac{4|K_1|}{3\mu_0 M_s} \quad (\text{Equation 15})$$

where  $f_r$  is the natural resonance frequency,  $\gamma$  is the gyromagnetic ratio,  $H_\alpha$  is the anisotropy energy,  $K_1$  is the anisotropy coefficient,  $\mu_0$  is the permeability of free space, and  $M_s$  is the saturation magnetization. Thus, the anisotropy energy determines the frequency of natural resonance. Meanwhile, Snoek's limit restricts the application of magnetic materials at high-frequency range, which can be described as a followed equation for isotropic ferromagnetic materials.<sup>65</sup>

$$(\mu_i - 1)f_r = \frac{1}{3\pi}\gamma M_s \quad (\text{Equation 16})$$

where  $\gamma M_s$  represents the Snoek constant and  $\mu_i$  is the initial permeability. For a given ferromagnetic material,  $M_s$  has a ceiling and  $\gamma$  is a constant. Thus, if  $f_r$  shifts to a higher frequency range, the  $\mu_i$  will inevitably decrease, resulting in a reduction of magnetic loss. Hence, the Snoek's limit restricts the application of ferromagnetic materials at high-frequency. Choosing soft magnetic metals with higher  $M_s$  values, such as Fe, Co, and Ni, is a considerable method to break the Snoek's limit.

### Interference cancellation principle

When the phase difference between the two electromagnetic waves reflected from the air-absorber interface and the absorber-metal back reflection interface is  $180^\circ$ , the two electromagnetic waves will interfere and cancel at the front interface of the monolayer absorber.<sup>84</sup> It can be expressed by the following equation.<sup>85</sup>

$$d_m = \frac{n\lambda}{4} = \frac{n c}{4f_m\sqrt{|\mu_r||\epsilon_r|}} (n = 1, 3, 5...) \quad (\text{Equation 17})$$

where  $d_m$  and  $f_m$  are the thickness and corresponding frequency of maximum RL values, respectively, and  $|\mu_r|$  and  $|\epsilon_r|$  are the modulus of complex permeability and permittivity at  $f_m$ , respectively. Using the interference cancellation principle, the optimal thickness that can achieve interference cancellation conditions at different frequencies can be designed, which is important for designing the matching thickness of the EMW absorbers. Most reports usually judge whether there exists interference cancellation by comparing the thickness calculated with the thickness obtained by the experiment tests.

## COMPOUNDING STRATEGY OF MOF DERIVATIVE COMPOSITE FOR EMW ABSORPTION APPLICATIONS

It is well known that MOF derivatives are widely used for EMW absorbing materials due to their advantages of large specific surface area, controllable structure, and high porosity.<sup>86</sup> Especially, magnetic MOF derivatives with both dielectric and magnetic loss can be prepared via simple calcination. Due to the existence of the periodic framework structure, the magnetic particles are uniformly distributed in the carbonized framework. The coordination of dielectric loss and magnetic loss endows the absorber with considerable EMW absorption performance. However, the magnetic porous carbon obtained by directly carbonizing the MOF suffers from poor impedance matching, a large filling amount, and a narrow EAB, which limits the

**Table 1.** EMW absorption performances of various graphene/MOF composites

Composite (precursor)	Filling ratio (wt %)	Minimum RL			Maximum EAB			Reference
		Value (dB)	Thickness (mm)	f <sub>m</sub> (GHz)	Value (GHz)	Thickness (mm)	Range (GHz)	
CeO <sub>2-x</sub> /RGO (Ce-MOF/GO)	50	-50.6	1.5	15.9	4.24	1.5	13.76-18	Li et al. <sup>60</sup>
Co/C-RGO (Co-MOF/GO)	6	-52	4.1	9.6	7.72	3.2	10.28-18	Zhang <sup>101</sup>
Co@C@RGO (Co-MOF/GO)	20	-67.5	2.6	8.8	5.4	2.0	10-15.4	Jinxiao et al. <sup>102</sup>
Co@NC@RGO (Co-MOF/GO)	50	-46.5	3.5	9.4	4.72	2.5	/	Liu et al. <sup>103</sup>
Fe-Co/NPC/RGO (Co-MOF/GO)	30	-52.9	2.5	10.1	3.1	2.5	8.6-11.7	Wang et al. <sup>104</sup>
CoNi@NCPs-rGO (ZIF-67@CoNi LDHs-GO)	30	-58.2	2.5	10.62	4.03	2.5	8.8-12.83	Zhao et al. <sup>105</sup>
CoNi@NC/rGO (CoNi-BTC/rGO)	25	-67.98	3.04	10.62	6.7	2.5	/	Xu et al. <sup>61</sup>
RGO/biMDPC (CoZn-MOF/rGO)	40	-33.8	3.7	8.8	4.2	3.4	8.2-12.4	Xiao et al. <sup>98</sup>
Co/ZnO/RGO (CZ-ZIF/GO)	8	-52.2	3.5	10.96	5.62	3.5	8.7-14.32	Liu et al. <sup>106</sup>
Fe-Co/NC/rGO (FeCo-MOF/GO)	8	-43.26	2.5	11.28	9.12	2.5	8.88-18	Wang et al. <sup>107</sup>
MCC/rGO (MIL-53/GO)	50	-62.53	2.66	8.8	11.68	3.6	6.32-18	Ding et al. <sup>62</sup>
Fe <sub>3</sub> O <sub>4</sub> /C/rGO (FeZn-MOFs/RGO)	20	-79	1.8	9.3	5.8	2.76	6.32-18	Shu et al. <sup>66</sup>
Ni/C@GF (Ni-MOF/GO)	15	-63	1.76	15.8	5.4	2.0	12.1-18	Wang et al. <sup>67</sup>
Zn-Co/C/RGO (ZnCo-MOF/GO)	20	-47.15	2.0	11.2	3.92	1.5	9.6-13.12	Wang et al. <sup>108</sup>
ZnO/ZnFe <sub>2</sub> O <sub>4</sub> /C@PG (ZnFe-MOF/PG)	25	-54.6	2.7	9.04	5.36	1.8	12.64-18	Song et al. <sup>47</sup>
NMC@GN (Ni-MIM/GO)	10	-53.99	3.9	4.82	4.39	1.4	9.6-13.12	Yi et al. <sup>78</sup>

practical application of such materials. The current study shows that compounding MOF derivatives with other types of materials is an effective way to optimize MOF-based EMW absorbing materials.

### MOF derivatives combined with graphene for EMW absorption

Nanocarbons are one type of most promising nanostructured materials due to their low density, chemical stability, tunable dielectric properties, and diverse forms.<sup>87-89</sup> Given its large specific surface area, residual defects, and oxygen-containing functional groups, reduced graphene oxide (RGO or rGO), which is an exceptional representative of carbon nanomaterials, is a leading choice for EMW absorbers.<sup>90-93</sup> Therein, graphene oxide (GO) is an ideal precursor for assembling monoliths with MOF nanocrystals for extended structures, such as thin films, aerogels, or foams.<sup>94-99</sup> However, due to the high conductivity and dielectric constant of graphene, the impedance matching is not satisfactory, resulting in strong skin reflection and weak attenuation for incident EMW.<sup>60,92,100</sup> An effective way to improve the EMW absorbing performance of graphene is to adjust the impedance matching by incorporating magnetic or other dielectric materials. The composite of graphene and other materials can not only achieve impedance matching but also have good loss capability to achieve excellent absorption performance.<sup>62</sup> When MOF derivatives are used to improve the impedance matching of graphene, more interfaces can increase the dielectric loss capability, while the inherent porous structure of MOFs can boost the multiple reflections of EMWs.<sup>67</sup> The addition of graphene can not only enable MOF derivative-based EMW absorbing materials with a lower filling fraction and a wider EAB but also enhance the mechanical properties of the composites.<sup>47</sup> The EMW absorption performances of various graphene/MOF composites are summarized in Table 1. There are typically two ways for combining graphene and MOFs, namely direct mixing and *in situ* growth.

#### Direct mixing method

In this method, MOF/graphene composites are prepared by simply mixing MOF crystals and graphene precursors. For instance, Li et al. prepared the composites of accordion-like CeO<sub>2-x</sub>/RGO based on the coordination of Ce-MOF and GO for tunable and optimized EMW absorption materials.<sup>60</sup> The RL<sub>min</sub> value of the composites is -50.6 dB when the mass ration of GO reaches 50%. The EAB reaches 4.24 GHz at a thickness of 1.5 mm. The excellent EMW absorption performance is attributed to the interfacial polarization between rGO sheets and CeO<sub>2-x</sub> NPs, the conductivity loss derived from the different conductivities of rGO and CeO<sub>2-x</sub>, and the 3D structure assembled from 2D rGO sheets prolonging the propagation

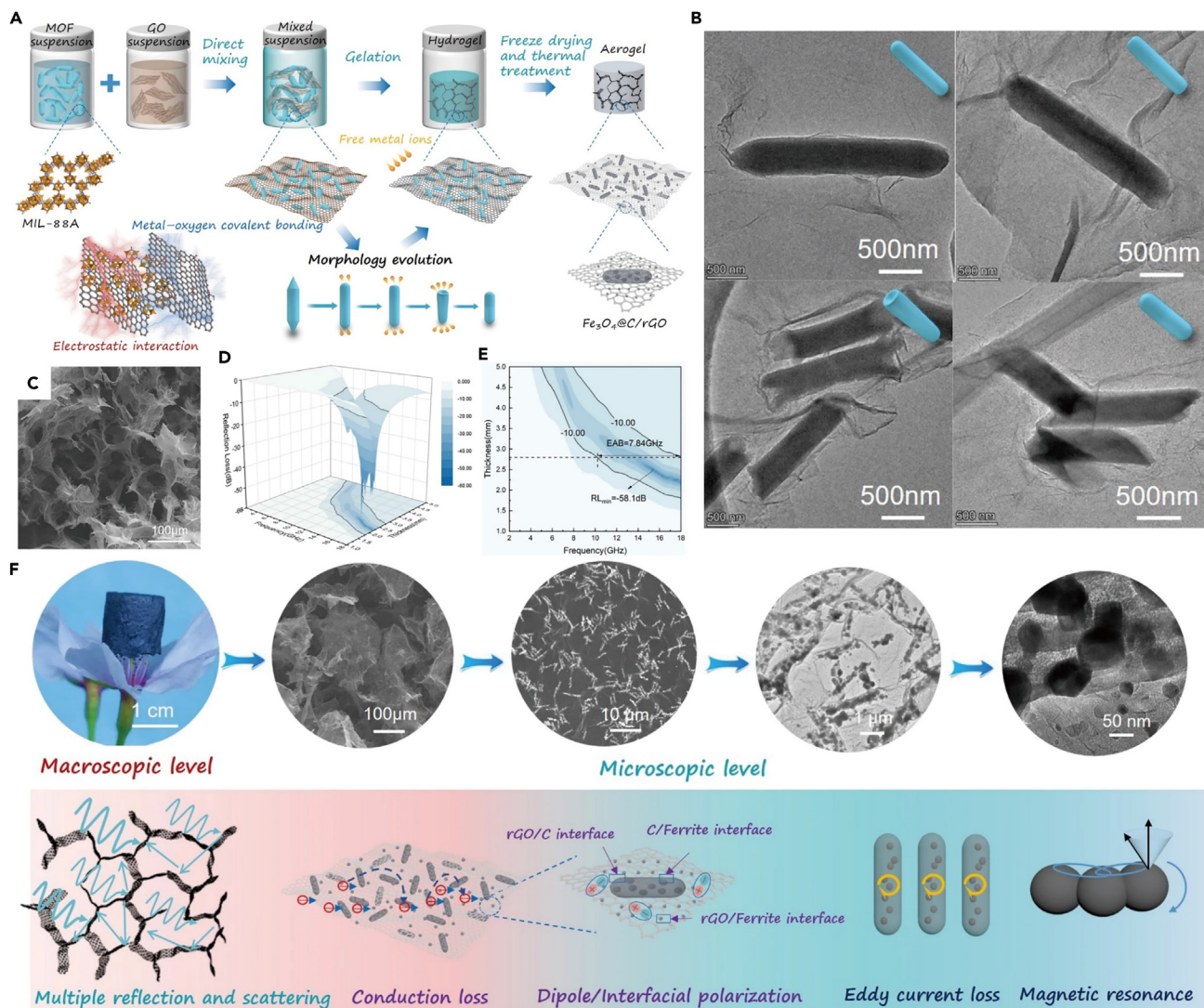


**Figure 2. The EMW absorption performance of MOF/rGO-derived magnetic and dielectric aerogels**

- (A) Schematic of the fabrication process of MOF/rGO hybrid aerogels.
- (B) Rod length distributions of MIL-88A/rGO aerogels prepared at different gelation times.
- (C) SEM of Ni-doped  $\text{Fe}_3\text{O}_4@\text{C}/\text{rGO}$ .
- (D and E) RL-f curves and EAB of  $\text{Fe}_3\text{O}_4@\text{C}/\text{rGO}$  aerogels.
- (F) Schematic of the associated EMW mechanism of the proposed MOF/rGO-derived magnetic and dielectric aerogels. Reprinted and adapted with permission from ref. <sup>48</sup>. Copyright 2022 Author (s).

path of EMW and improving multiple scattering and reflections. Fan et al. synthesized RGO/bimetallic-MOF-derived carbon with  $RL_{\min}$  of  $-33.8$  dB and EAB of  $4.2$  GHz.<sup>109</sup> Wang et al. synthesized Zn-Co/C/RGO with  $RL_{\min}$  of  $-47.15$  dB and EAB of  $3.93$  GHz.<sup>108</sup>

Graphene aerogels are widely used in the field of EMW absorption due to their high porosity and low density. Not only can the pores in the graphene aerogel improve the impedance matching but they can also perform multiple reflections or scattering of the EMW to enhance the EMW absorption performance. The current study shows that the combination of magnetic MOF and graphene aerogel can promote the gelation of graphene due to the opposite potentials of GO and MOF particles while adding additional magnetic loss.<sup>48,110</sup> Moreover, the interactions between MOF and GO lead to the uniform dispersion of MOF. Huang et al. prepared Ni-doped  $\text{Fe}_3\text{O}_4@\text{C}/\text{rGO}$  aerogels by the MOF-induced GO gelation into aerogels followed by carbonization as shown in Figure 2.<sup>48</sup> At an ultra-low loading of  $0.6$  wt %, the  $RL_{\min}$

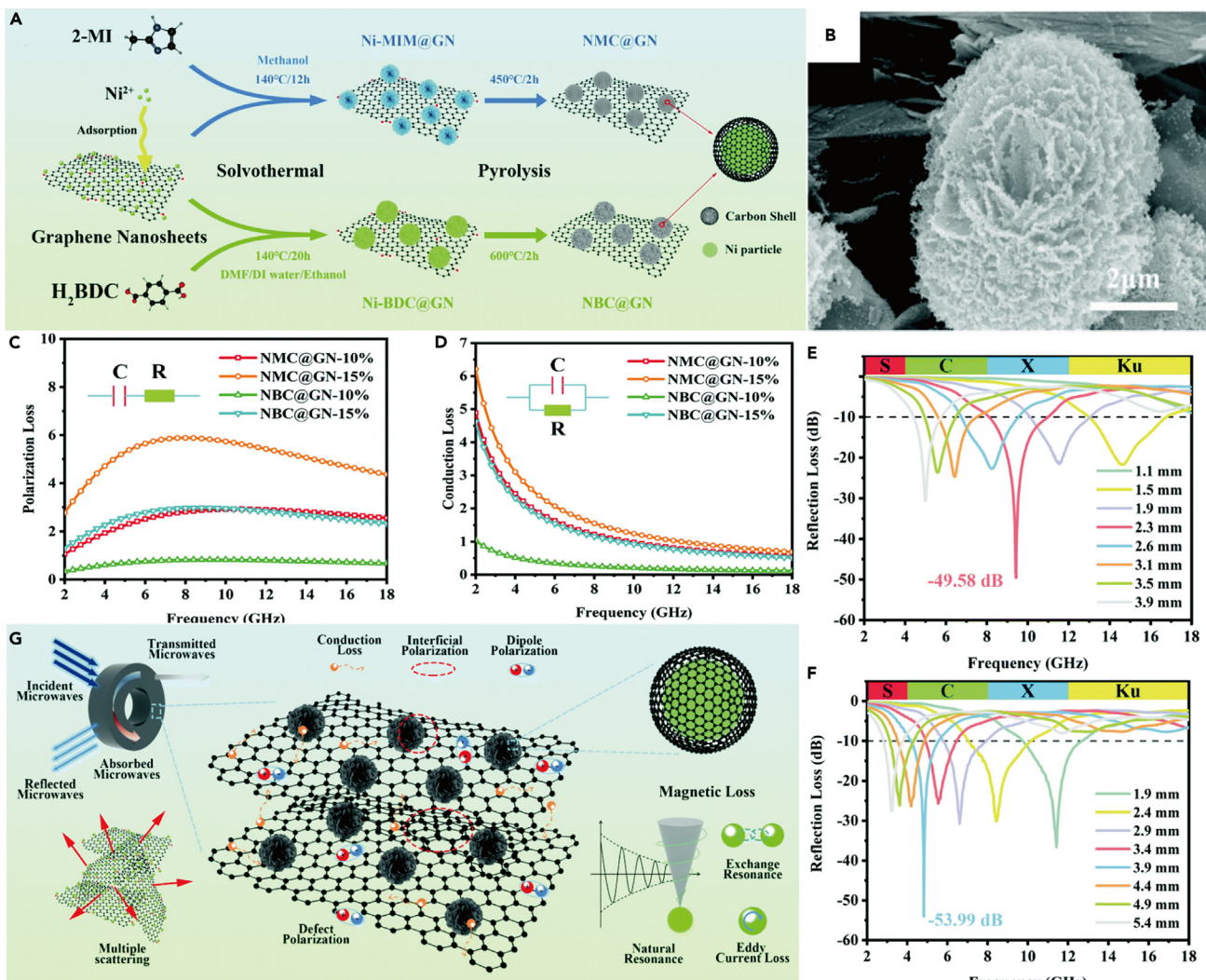


**Figure 3. The EMW absorption performance of NMC@GN and NBC@GN**

(A) Schematic illustration of the fabrication process of NMC@GN and NBC@GN.

(B) SEM images of NBC@GN.

(C and D) Conduction loss and polarization loss of NMC@GN and NBC@GN.

(E and F) Reflection loss with different thicknesses of NBC@GN and NMC@GN.

(G) Possible EMW attenuation mechanism of the composites. Reprinted and adapted with permission from ref.<sup>78</sup> Copyright 2021 Royal Society of Chemistry.

reached -59 dB at 2.85 mm and the EAB reached 7.92 GHz at 2.8 mm. The excellent EMW absorption performance is attributed to the synergistic effect of impedance matching and attenuation capability derived from the rational design of components and porous structure. Yu et al. prepared Ni<sub>3</sub>S<sub>2</sub>@NSGA (Ni<sub>3</sub>S<sub>2</sub>@N, S-codoped graphene aerogel) aerogels in the same method.<sup>110</sup> At an ultra-low loading of 1.75 wt %, the RL<sub>min</sub> value reached -46.9 dB at 17.1 GHz and the EAB reached 6.3 GHz with a thickness of 2.38 mm. Excellent EMW absorption properties are attributed to the coordinated coordination of multi-component and porous structure.

### In situ MOF synthesis

Another way to prepare MOF/graphene composites is by anchoring metal ions on the surface of graphene by electrostatic interaction, and then synthesizing MOFs *in situ* on the graphene surface by adding organic ligands. For instance, Yi et al. grew two novel petaloid nickel-based MOFs (denoted as Ni-MIM and Ni-BDC) on the surface of graphene nanosheets by a hydrothermal method as shown in Figure 3, two

**Table 2.** EMW absorption performances of various CNTs/MOF composites

Composite (precursor)	Filling ratio (wt%)	Minimum RL			Maximum EAB			Ref
		Value (dB)	Thickness (mm)	f <sub>m</sub> (GHz)	Value (GHz)	Thickness (mm)	Range (GHz)	
Co-C/MWCNTs (Co-MOF/MWCNTs)	15	-48.9	2.99	/	/	/	/	Yin et al. <sup>63</sup>
Co-C/MWCNTs (Co-MOF/MWCNTs)	20	-33.4	6.0	/	3.8	/	10.8–14.6	Zhang et al. <sup>111</sup>
CoFe <sub>2</sub> O <sub>4</sub> @CNTs (CoFe-MOF/CNTs)	40	-34.6	2.5	13.4	7.1	2.5	10.0–17.1	Liu et al. <sup>116</sup>
Co/MWCNTs (Co-MOF/MNWCTs)	10	-50.2	1.84	14.3	4.3	1.84	12.3–16.6	Lu et al. <sup>120</sup>
CBM 70.29.1 (Co-MOF/MNWCTs/BAM)	55	-26	2.5	12.4	4.32	2.2	8.2–12.4	Peibo et al. <sup>121</sup>
Co-C/MWCNTs (CoZn-MOF/MNWCTs)	25	-50	2.4	/	4.3	1.8	/	Shu et al. <sup>85</sup>
MW/MOF (FeCoNi-MOF/MNWCTs)	30	-36	2.0	8.7	5.0	2.0	/	Mirzaee et al. <sup>122</sup>
CNT/FeCoNi@C (FeCoNi-MOF/MNWCTs)	30	-57.1	3.0	/	6.8	1.0	/	Hu et al. <sup>49</sup>
CNT/MOF (Ni-MOF/CNT)	25	-24.32	5.0	4.5	/	/	/	Liu et al. <sup>103</sup>
ZnO@MWCNTs (Zn-MOF/MNWCTs)	20	-47.4	2.7	7.68	3.7	1.5	/	Li et al. <sup>50</sup>

absorbers of NMC (MOF derivatives derived from Ni-MIM)@GN and NBC (MOF derivatives derived from Ni-BDC)@graphene (GN) were obtained after calcination treatment.<sup>78</sup> The corresponding EMW absorbing performance was deeply analyzed by changing the filling ratio of the absorber in the matrix. The RL<sub>min</sub> value of NMC@GN reached -53.99 dB at 4.82 GHz under a low load of 10 wt % and the EAB was 4.39 GHz. The RL<sub>min</sub> value of NBC@GN reached -49.58 dB at 9.42 GHz. The extraordinary EMW absorption performance mainly came from four parts: the unique petal-like porous carbon framework of MOFs, the three-dimensional (3D) conductive network formed by the connection of GNs, the polarization process between the interfaces of multiple heteroelements, and the impedance matching derived from the magnetic Ni. By a similar synthesis, Wang et al. prepared FeCo-MOF/rGO composites by *in situ* growth of MOF on silkworm chrysalis-like graphene.<sup>107</sup> FeCo-MOF/rGO composites were transformed into Fe-Co/Ni/N-doped carbon (NC)/rGO composites with a hierarchical pore structure after high-temperature carbonization.<sup>107</sup> The composites had an ultra-wide EAB of 9.12 (8.88–18) GHz at a low loading of 8%. Shu et al. prepared Fe<sub>3</sub>O<sub>4</sub>/C/rGO composites by growing *in situ* FeZn-MOFs on the GO sheets and followed by carbonization approach.<sup>66</sup> The RL<sub>min</sub> reached -79 dB at 9.8 GHz with a thickness of 1.8 mm. The EAB reached 5.8 (6.32–18) GHz at 2.76 mm. Song et al. prepared ZnO/ZnFe<sub>2</sub>O<sub>4</sub>/C@porous graphene (PG) composites using ZnFe-MOF/PG as a precursor.<sup>47</sup> The RL<sub>min</sub> reached -54.6 dB at 9.04 GHz, and EAB reached 5.36 GHz with a thickness of 1.8 mm. Summed up, *in situ* growth has better uniformity, but direct mixing can better control the relative ratio of graphene and MOFs and can extend more functions of MOFs, such as promoting the gelling and crosslinking of graphene.

The combination of graphene and MOF derivatives has great advantages in improving conductive loss and optimizing interfacial polarization, in filling ratio when forming aerogels with integrated structure and function. In addition, the functional groups of graphene can induce polarization loss as polarization centers. However, the high conductivity of graphene often leads to impedance matching.

### MOF derivatives combined with CNTs for EMW absorption

Owing to their light weight, high conductivity, and large aspect ratio and specific surface area, CNTs are widely used in preparing EMW absorbing materials with significant conduction loss.<sup>111</sup> Nevertheless, the single-component CNT absorber has poor matching and a large matching thickness as a result of excessive conductivity and a single loss mechanism, which limits its further development in the field of EMW absorption.<sup>112–115</sup> Moreover, it is difficult for CNTs with low magnetic loss to obtain better impedance matching by directly tuning the loss mechanism.<sup>116–119</sup> Therefore, introducing additional magnetic particles has become an effective way to improve the EMW absorbing properties of CNTs. Therein, the introduction of magnetic MOF derivatives has greater advantages than the direct introduction of conventional magnetic particles. Particularly, constructing the 3D electromagnetic network composed of MOF derivatives as nodes and CNTs as wires is beneficial for improving impedance matching and loss capability. The EMW absorption performances of various CNTs/MOF composites are summarized in Table 2. Compared with graphene, 1D CNTs can better connect the MOF particles, thus avoiding agglomeration, which can reduce the filling amount.

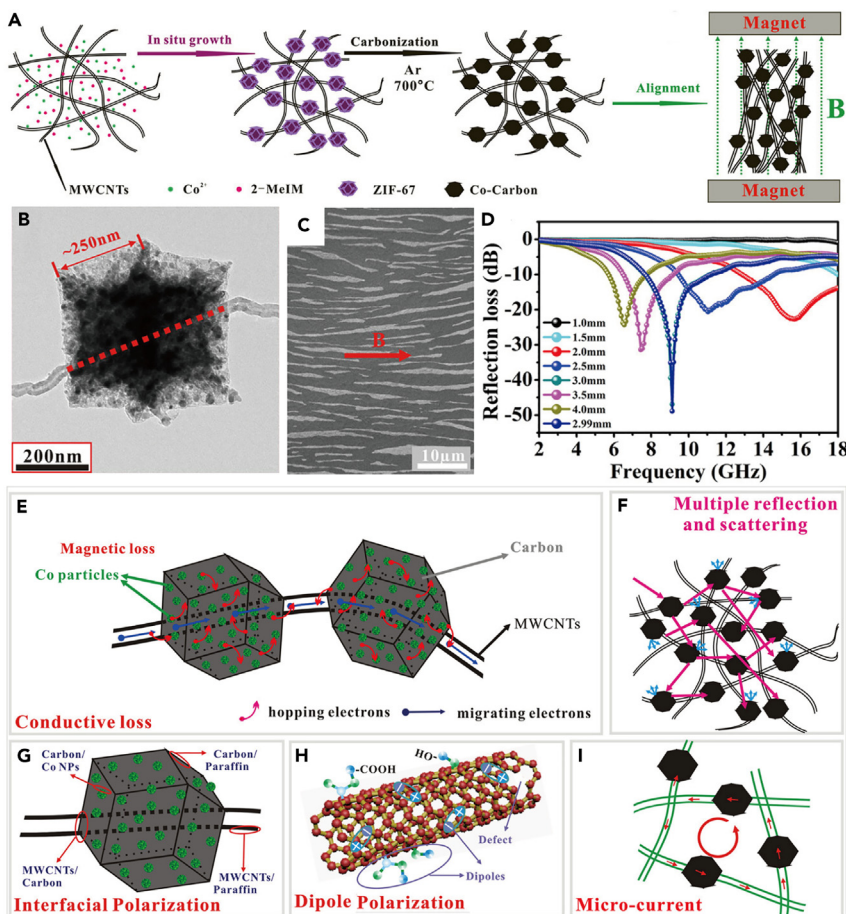


**Figure 4. The EMW absorption performance of alignment Co-C/MWCNTs**

- (A) Synthesis of Co-C/MWCNTs and alignment of Co-C/MWCNTs in paraffin matrix under an external magnetic field.
- (B) TEM image of Co-C/MWCNTs composite.
- (C) SEM image of Co-C/MWCNTs dispersed in paraffin with a magnetic field.
- (D) Reflection loss of oriented Co-C/MWCNTs composite.
- (E–I) Scheme of primary EMW attenuation models of Co-C/MWCNTs composite. Reprinted and adapted with permission from ref.<sup>63</sup> Copyright 2017 American Chemical Society.

Co-based MOFs are most widely used among MOF-based EMW absorbing materials, and thus a series of Co-MOF/CNTs composites have been prepared for EMW absorbers.<sup>63,111,120,123</sup> For example, Yin et al. used multi-walled CNTs (MWCNTs) as templates for ZIFs growth and obtained the Co-C/MWCNTs composites by pyrolysis as shown in Figure 4<sup>63</sup>. ZIF-derived Co-C porous particles were interconnected by MWCNTs, building a conductive network for electron hopping and migration. The alignment of the Co-C/MWCNTs composite in the paraffin mechanism was adjusted by applying an external magnetic field so that the MWCNTs were aligned along the direction of the magnetic field. At 15% filling ratio, the  $RL_{min}$  reached  $-48.9$  dB with a thickness of 2.99 mm. The excellent EMW absorption properties benefited from the conductive network, directionally enhanced dielectric loss, and synergistic effects between the magnetic and dielectric components. Hu et al. used Fe-doped CNTs and FeCoNi-MOF as precursors to obtain CNT/FeCoNi-@C composites after calcination at different temperatures.<sup>49</sup> The  $RL_{min}$  reached  $-51.7$  dB with a thickness of 3 mm, and the EAB reached 6.8 GHz with a thickness of 1.0 mm. Similarly, a series of N-doped porous Co-C/MWCNTs nanocomposites with different MWCNT contents were prepared by calcination at 700°C using CoZn-MOF/MWCNTs as a precursor by Shu et al.<sup>85</sup> The  $RL_{min}$  reached  $-50$  dB with a thickness of 2.4 mm and the EAB reached 4.3 GHz with a thickness of 1.8 mm. The excellent EMW absorption performance can be attributed to the synergistic effect of porous structure, dipole, and interfacial polarization, dielectric loss, magnetic loss, excellent impedance matching, and good electromagnetic attenuation capability.

**Table 3.** EMW absorption performances of various BDC/MOF composites

Composite (precursor)	Filling ratio (wt%)	Minimum RL			Maximum EAB			Reference
		Value (dB)	Thickness (mm)	f <sub>m</sub> (GHz)	Value (GHz)	Thickness (mm)	Range (GHz)	
Carbon-cotton/Co@NPC (Biomass cotton/Co-MOF)	25	-60	2.55	8.48	4.4	1.65	/	Zhao et al. <sup>55</sup>
HCF@CZ-CNT (Biomass cotton/Co-MOF)	10	-53.3	2.9	7.8	8.02	2.0	9.98–18	Yang et al. <sup>80</sup>
N-Ni-Co <sub>x</sub> S <sub>y</sub> /Ni <sub>x</sub> S <sub>y</sub> @C (ZIF-67/S-Ni(II)-CMC)	25	-48.3	2.0	11.7	3.9	1.5	14.0–17.9	Song et al. <sup>82</sup>
FeCo/C@WC (ZIF-67/Fe <sub>3</sub> O <sub>4</sub> /WA)	15	-47.6	1.5	15.7	8.9	1.96	9.1–18	Zhao et al. <sup>56</sup>
Ni/NC/C (Ni-MOF/Loofah)	16	-63.1	2.0	13.84	5.1	2.0	11.3–16.4	Zhou et al. <sup>145</sup>
MPC@Ni/C (Ni-MOF/The pine nutshell)	20	-73.8	2.2	16.3	5.8	2.2	12.2–18	Di et al. <sup>146</sup>
Co@C/C sheets (CoZn-MOF/Oroxylum indicum)	12	-66.9	1.66	/	5.6	1.9	9.8–15.3	Zhang et al. <sup>124</sup>

1D CNTs as wires can connect MOF derivatives to construct the 3D electromagnetic network, which is beneficial for improving the dispersion of MOF derivatives and their loss capability. The functional groups of CNTs can induce polarization loss as polarization centers as well as graphene. CNTs also face the problem of impedance not being easily matched due to high conductivity, but the problem is not as serious as with graphene due to the zero bandgap of graphene.

### MOF derivatives combined with BDC for EMW absorption

The complex preparation process and high cost of carbon materials such as graphene and CNTs hinder their manufacture and application in EMW absorbing fields.<sup>124,125</sup> Therefore, it is imperative to discover alternatives for cost reduction and mass production. BDCs have received extensive attention due to their low cost, environmental friendliness, sustainability, ease of manufacture, and non-toxicity.<sup>126–134</sup> In addition, BDCs can maintain their natural morphology after the carbonization process, including large specific surface area, porous structure, hierarchical structure, and hollow structure, which is advantageous for boosting the attenuation of EMWs.<sup>84,135–138</sup> Up to now, biomass materials such as carbonized spinach stems,<sup>139</sup> wood,<sup>137</sup> walnut shells,<sup>140</sup> loofah sponges,<sup>141</sup> rice,<sup>142</sup> eggshell membranes,<sup>143</sup> and waxberries<sup>144</sup> have been reported to be widely used in EMW absorbing materials. Using BDC as the substrate for MOF deposition, on the one hand, the hierarchical porosity and other features inherited from biomass materials will enhance the loss of EMW, on the other hand, the self-agglomeration of MOF can be effectively prevented, thus ensuring the uniform dispersion of NPs. Furthermore, the synergistic effect of dielectric loss and magnetic loss not only optimizes impedance matching but also facilitates loss capability. The combination of biomass and MOF provides a low-cost and sustainable strategy for the preparation of lightweight EMW absorbers with excellent absorption properties. As summarized in Table 3, the EMW absorption performances of various BDC/MOF composites were significantly improved due to optimized impedance matching and multiple reflection and scattering based on the hierarchical porous structure of BDC.

Cotton is used to prepare EMW absorbing materials due to its unique hierarchical macro- and microporous structure.<sup>55,80</sup> Yang et al. prepared layered hollow carbon fibers by calcining hollow cotton fibers coated with Co-MOF as shown in Figure 5<sup>80</sup>. Due to the layered fiber structure and the synergistic effect of polarization relaxation and magnetic loss, the EAB of composite reached 8.02 GHz at 2.0 mm. Zhao et al. deposited ZIF-67 particles on cotton as a substrate for the development of carbon cotton/Co@nanopores carbon (NPC) absorbers.<sup>55</sup> The prepared composites showed superior EMW absorption performance than the MOF derivative Co@NPC due to better impedance matching after calcination at 700°C. The RL<sub>min</sub> reached -60 dB at 8.48 GHz. Carboxymethyl cellulose sodium (CMC-Na) derived from natural cellulose has the advantages of good biocompatibility, low cost, good biocompatibility, rich functional groups, etc. Song et al. prepared N-Ni-Co<sub>x</sub>S<sub>y</sub>/Ni<sub>x</sub>S<sub>y</sub>@C composites by annealing ZIF-67 with thiourea-infiltrated CMC-Ni beads at high temperatures.<sup>82</sup> The synergistic effect of *in situ* vulcanized ZIF-67 and CMC (carboxymethyl cellulose) not only prevented the aggregation of magnetic components but also improved the impedance matching of carbon materials.

Wood can achieve anisotropy due to the uneven shape, size, and distribution of pores. As such, wood offers a wide variety of design alternatives for layered porous materials.<sup>137</sup> Xiong et al. prepared a tomato-like

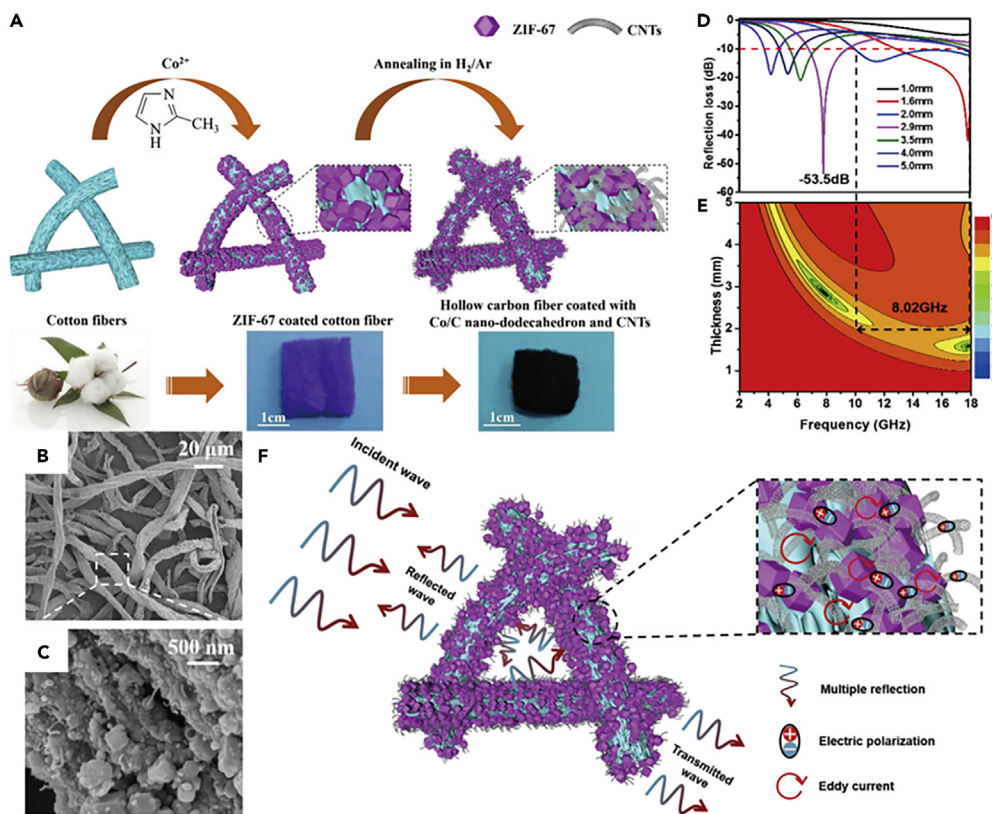


**Figure 5. The EMW absorption performance of HCF@CZ-CNT (Hierarchical carbon fiber coated with Co/C nano-dodecahedron particles where CNTs were anchored)**

(A) Schematic illustration of the synthesis procedure for HCF@CZ-CNT.

(B and C) SEM images for HCF@CZ-CNT.

(D and E) Reflection loss curves and the corresponding 2D contour plots of HCF@CZ-CNT.

(F) Possible EM wave attenuation mechanisms HCF@CZ-CNT. Reprinted and adapted with permission from ref.<sup>80</sup>

Copyright Elsevier Inc.

hierarchical porous FeCo/C@ wood carbon aerogel using natural wood, ZIF-67, and  $\text{Fe}_3\text{O}_4$  as raw materials.<sup>56</sup> Compared with single-pore structures assembled from 1D/2D materials, hierarchical porous structures derived from natural wood and MOFs had the synergistic advantage of multi-scale building blocks, which can provide better performance. The combination of the macroporous wood shell and mesoporous carbon nanocages provided an excellent hierarchical dielectric network for the composite. The uniformly dispersed FeCo NPs enhanced the magnetic loss of carbonaceous substrates. The  $\text{RL}_{\min}$  reached  $-47.6$  dB at 1.5 mm, and the EAB reached 8.9 GHz at 1.96 mm. Zhou et al. used Ni-MOF and loofah plants as precursors to prepare "tree flower" NC/carbon (C) composites by *in situ* pyrolysis under an argon atmosphere.<sup>145</sup> The  $\text{RL}_{\min}$  of Ni/NC/C reached  $-63$ . dB. Zhang et al. used 2D ZnCo-MOF and *Oroxylum indicum* as precursors to prepare a Co@C/C composite with a hierarchically porous structure and large specific surface area by hydrothermal and pyrolysis for EMW absorption.<sup>124</sup> The optimal RL value reached  $-66.9$  dB at 1.66 mm and the EAB reached 5.6 GHz at 1.9 mm.

The advantage of BDC is that it can inherit the multi-level structure of natural materials after carbonization, which is conducive to impedance matching and improved loss capability through multiple reflections and scattering. In addition, compared with materials such as graphene and CNTs, BDC comes from a wide range of sources, which can significantly reduce the production cost of EMW-absorbing materials.

### MOF derivatives combined with MXene for EMW absorption

MXenes, as typical two-dimensional materials, have been widely used due to their low density, large specific surface area, good conductivity, and unique accordion structure.<sup>84,147–151</sup> MXenes are usually obtained

**Table 4.** EMW absorption performances of various MXenes/MOF composites

Composite (precursor)	Filling ratio (wt%)	Minimum RL			Maximum EAB			Reference
		Value (dB)	Thickness (mm)	f <sub>m</sub> (GHz)	Value (GHz)	Thickness (mm)	Range (GHz)	
Ti <sub>3</sub> CNT <sub>x</sub> /HCF (Co-MOF/Ti <sub>3</sub> CNT <sub>x</sub> )	15	-55.2	1.43	13.4	4.4	1.43	13.6–18	Cai et al. <sup>79</sup>
CFMM (CoFe-MOF/Ti <sub>3</sub> C <sub>2</sub> T <sub>x</sub> )	50	/	/	/	6.1	2.0	/	Li et al. <sup>50</sup>
MXene/Co-CZIF (Co-MOF/Ti <sub>3</sub> C <sub>2</sub> T <sub>x</sub> )	50	-60.09	2.7	7.36	9.3	2.7	/	Han et al. <sup>52</sup>
MXene/Ni-CZIF (Ni-MOF/Ti <sub>3</sub> C <sub>2</sub> T <sub>x</sub> )	50	-64.11	3.4	5.12	4.56	3.4	/	Han et al. <sup>52</sup>
Co/TiO <sub>2</sub> -C (Co-MOF/Ti <sub>3</sub> C <sub>2</sub> T <sub>x</sub> )	45	-41.1	3.0	9.0	4.04	2.0	/	Wang et al. <sup>156</sup>
Co/CNTs-MXene@CF (Co-MOF/Mxene/CF)	10	-64.61	2.52	/	5.04	1.5	/	Wang et al. <sup>154</sup>
MMC (CoNi-MOF/MXene)	50	-51.6	1.6	15.1	4.5	1.6	13.2–17.7	Wu et al. <sup>157</sup>
MXene/CoNi/N-CNTs (CoNi-MOF/MXene)	30	-52.64	3.8	3.12	0.72	3.8	2.8–3.52	Zhou et al. <sup>71</sup>
CN1OT (CoNi-MOF/MXene)	5	-47.17	2.9	/	5.44	2.9	/	Wang et al. <sup>84</sup>
TMOT (CoNi-MOF/MXene)	5	-67.22	1.7	/	3.84	1.7	/	Wang et al. <sup>72</sup>
Fe&TiO <sub>2</sub> @C (MXene/Fe-MOFs)	50	-51.8	3.0	6.6	6.5	1.6	/	Deng et al. <sup>83</sup>

by selectively etching certain atoms in the MAX phase.<sup>152,153</sup> The excellent conductivity of MXenes and the dipole polarization induced by abundant surface terminating functional groups (e.g., -O, -OH, and -F) are favorable for the formation of dielectric loss.<sup>51,71,154,155</sup> The accordion structure facilitates multiple scattering of EMW.<sup>156</sup> On the one hand, the weak magnetic properties and excessively high electrical conductivity of the laminated MXene sheets lead to impedance mismatching, on the other hand, due to the van der Waals force and hydrogen bonding, the 2D MXene sheets have the phenomenon of agglomeration and self-stacking, which seriously reduces the effective surface and electron transport speed.<sup>157</sup> To simultaneously address the above mentioned issues, researchers typically introduce magnetic particles between 2D MXene sheets.<sup>158,159</sup> Compared with conventional magnetic particles, the introduction of magnetic MOF derivatives can generate more heterointerfaces, and the structural designability of MOFs (such as hollow cores) is beneficial to optimizing EMW absorption performance.<sup>30,42,160</sup> Therefore, the combination of magnetic MOF derivatives with MXene is an effective way to prepare high-performance EMW absorption materials. The EMW absorption performances of various MXene/MOF composites are summarized in Table 4, and the large permittivity caused by the high conductivity of MXene gives it a great advantage in the field of low-frequency absorption.

Deng et al. constructed sandwich-like 2D layered Fe&TiO<sub>2</sub>@C nanocomposites derived from MXene/Fe-MOFs hybrids via a fast microwave-assisted heating reaction and appropriate thermal treatment as shown in Figures 6A - 6D.<sup>83</sup> Fe and TiO<sub>2</sub> particles were generated *in situ* between the MXene-derived carbon sheets during the thermal treatment, which enriched the heterointerface. Due to the high interfacial polarization and the synergistic cooperation of the EMW attenuation mechanisms, Fe&TiO<sub>2</sub>@C nanocomposites exhibited strong electromagnetic energy attenuation and good impedance matching. The RL<sub>min</sub> reached -51.8 dB. To achieve the purpose of low-frequency absorption and selective absorption, Zhou et al. reported a 3D heterostructure constructed from multi-dimensional components (MXene/CoNi/N-CNTs) for low-frequency microwave absorption as shown in Figures 6E - 6J.<sup>71</sup> The optimal absorption peak could be adjusted between the S-band and the C-band by adjusting the content of alloy components. The RL<sub>min</sub> value was around -50 dB in both S-band and C-band which exhibited excellent low-frequency absorption performance. The MOF-derived 1D N-CNTs acted as bridges to connect the MXene and CoNi alloys while serving as the basic unit of the 3D conductive network, greatly enhancing the path of the excited-state electronic transitions. In addition, the multi-components formed abundant interfaces, which facilitated interface polarization. Wang et al. constructed hierarchical Co/CNTs-MXene@CF (Co/CNTs-MXene@cotton fiber) heterostructure composites derived from vertical Co-ZIF nanosheet arrays via self-assembly process and thermocatalytic treatment.<sup>154</sup> The RL<sub>min</sub> reached -64.61 dB at 2.52 mm, and the EAB was 5.04 GHz. Wang et al. synthesized MOF derivatives/MXene cross-linked network by linking flower-like MOF derivatives and 2D flexible MXene sheets.<sup>84</sup> At a low fill of 5 wt %, the RL<sub>min</sub> reached -47.17 dB at 2.9 mm. Wu et al. fabricated MOF-loaded MXene fibers by electrostatic self-assembly and used a one-step catalytic self-deposition (CSD) method to construct double 1D heterostructures for EMW absorption.<sup>157</sup> At a thickness of 1.6 mm, the RL<sub>min</sub> reached -51.6 dB.

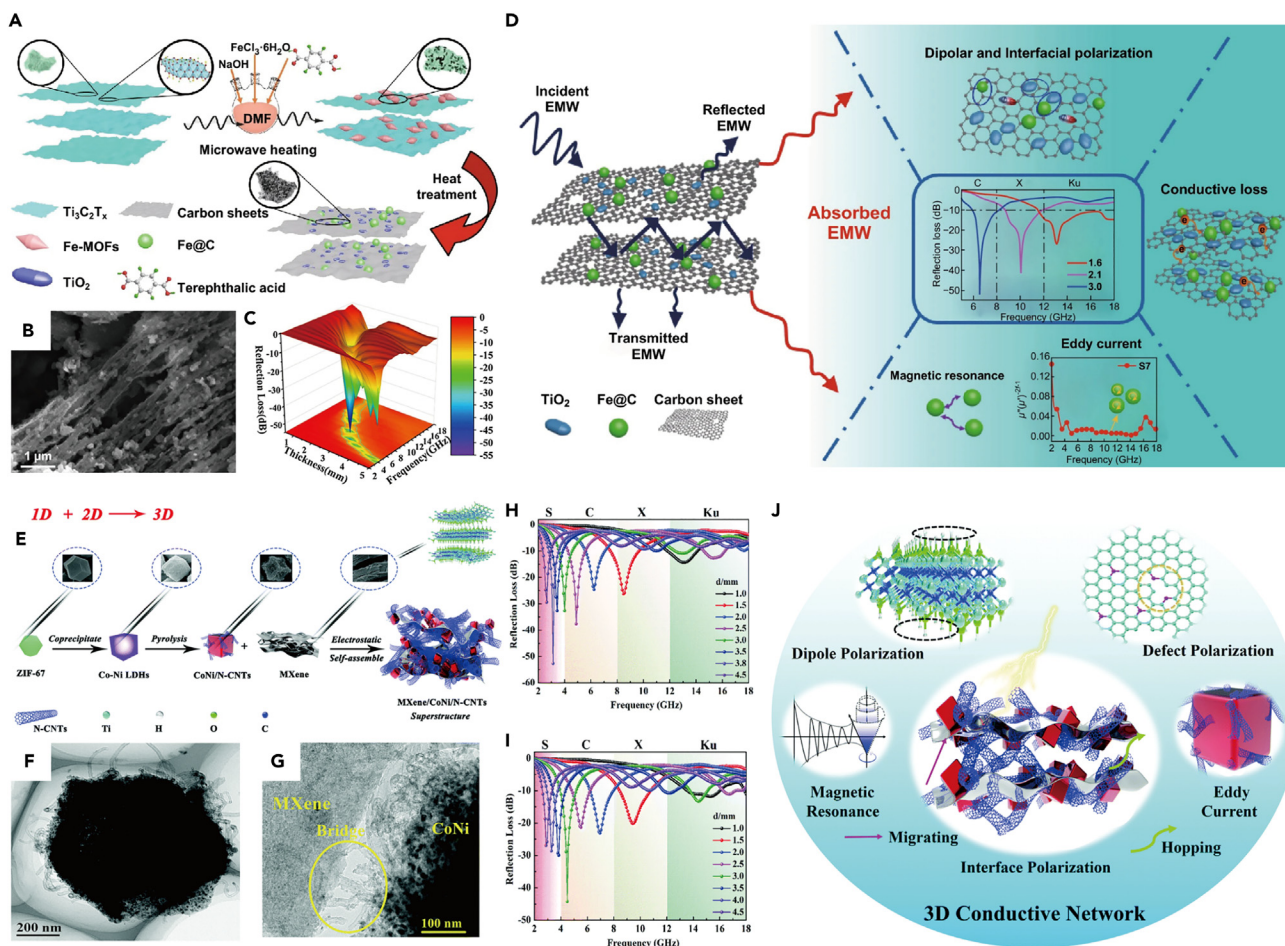


**Figure 6. The EMW absorption performance of Fe&TiO<sub>2</sub>@C and MXene/CoNi/N-CNT**

(A) Schematic representation of the facile synthesis route of the Fe&TiO<sub>2</sub>@C.

(B) SEM image of Fe&TiO<sub>2</sub>@C.

(C) 3D maps of RL values for Fe&TiO<sub>2</sub>@C at different thicknesses over 2–18 GHz.

(D) Illustration of EMW absorption mechanisms for Fe&TiO<sub>2</sub>@C nanocomposites. Reprinted and adapted with permission from ref.<sup>83</sup> Copyright 2020 Author (s).

(E) Schematic illustration of the synthesis process of the MXene/CoNi/N-CNT superstructure.

(F and G) TEM images of MXene/CoNi/N-CNT.

(H and I) RL curves of the samples.

(J) Schematic diagrams of the potential microwave absorption mechanisms of MXene/CoNi/N-CNTs. Reprinted and adapted with permission from ref.<sup>71</sup> Copyright 2022 Royal Society of Chemistry.

The hollow structure not only played a crucial part in realizing lightweight EMW absorption but also served as a medium to balance the impedance between the absorber and air, allowing the EMW absorption performance to be precisely tuned.<sup>87,161,162</sup> Wang et al. prepared hollow NiCo compound@MXene networks by etching ZIF (Zeolitic imidazolate framework) 67 templates and subsequently anchoring Ti<sub>3</sub>C<sub>2</sub>T<sub>x</sub> nanosheets via electrostatic self-assembly as shown in Figure 7<sup>72</sup>. The electromagnetic parameters of the composites were adjusted by changing the amount of MXene. The layered structure effectively prevented the stacking of 2D MXene sheets, which was beneficial to enhancing the conduction loss and increasing the effective surface area. Based on the synergistic effect of multiple components and special structures, the composite exhibited excellent EMW absorption properties. When the amount of MXene was 9.0 mL (1 mg/mL), LDHT-9 reached an EAB of 6.72 GHz. The RL<sub>min</sub> of TMOT-21 reached -67.22 at a thickness of 1.7 mm obtained by calcining LDHT-21 at 350°C in an argon atmosphere. It indicates that the combination of MXene with hollow structures is a promising effective candidate for the development of ultralight and ultrathin EMW absorbing materials.

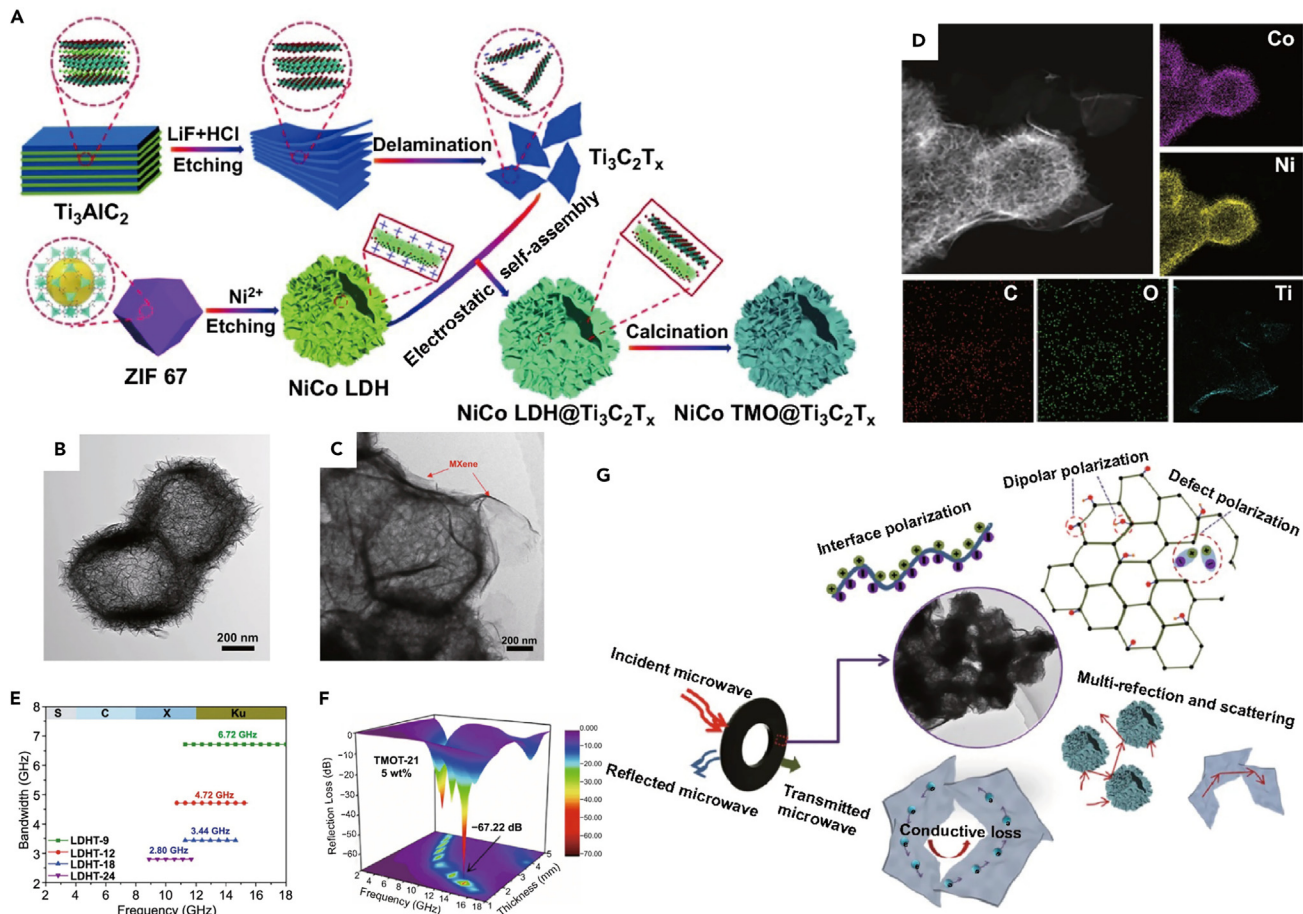


**Figure 7. The EMW absorption performance of LDHT (NiCo layered double hydroxides@ $\text{Ti}_3\text{C}_2\text{T}_x$ ) and TMOT (After calcination, transition metal oxide@ $\text{Ti}_3\text{C}_2\text{T}_x$ )**

(A) Schematic diagram of synthetic process for LDHT and TMOT.

(B and C) TEM images of NiCoLDH nanocage and LDHT.

(D) Element mapping images of TMOT.

(E) EAB with the filler content of 15 wt% of LDHT.

(F) 3D plots of RL value for TMOT.

(G) Schematic illustration of microwave absorption mechanism for TMOT. Reprinted and adapted with permission from ref.<sup>72</sup> Copyright 2021 Author(s).

As a highly conductive material, Mxene is able to improve the conductive loss capacity of MOF derivatives. In addition, a high dielectric constant is beneficial to the research and development of low-frequency absorbing materials. However, the problem of oxidation limits its further practical applications.

### MOF derivatives combined with conductive polymers for EMW absorption

Conductive polymers are a class of widely used dielectric loss EMW absorbing materials based on the three characteristics.<sup>163</sup> Firstly, the conductivity of conductive polymers can vary between insulators, semiconductors, and metal conductors, satisfying various requirements for the conductivity of EMW absorbing materials. Conductive polymers in the semiconductor state can not only provide conductive loss but also avoid the skin effect caused by excessive conductivity. Secondly, conductive polymers have the characteristics of low density, which is typically between 1.0 and 2.0 g/cm<sup>3</sup>. Thirdly, conductive polymers have good thermal stability and environmental stability. Due to the advantages of the simple synthesis process, low density, good conductivity, corrosion resistance, and stable chemical properties, polypyrrole (PPy) and polyaniline (PANI) are two kinds of conductive polymers that are widely used.<sup>164-169</sup> Based on the advantages of conductive polymers, the combination of conductive polymers and MOF derivatives can be used to enhance the conductive loss capability while optimizing the impedance matching of MOF derivative-based EMW absorbing materials.<sup>170</sup> The EMW absorption performances of various conductive polymers/MOF

**Table 5.** EMW absorption performances of various conductive polymers/MOF composites

Composite (precursor)	Filling ratio (wt %)	Minimum RL			Maximum EAB			Reference
		Value (dB)	Thickness (mm)	f <sub>m</sub> (GHz)	Value (GHz)	Thickness (mm)	Range (GHz)	
Co <sub>3</sub> O <sub>4</sub> @PANI (Co-MOF/PANI)	50	-37.39	4.0	7.28	3.52	3.0	/	Jia et al. <sup>64</sup>
Co/C@PPy (Co-MOF/PPy)	10	-44.76	2.0	17.32	6.6	2.5	11.0–17.6	Sun et al. <sup>171</sup>
CoZn/C@MoS <sub>2</sub> @PPy (CoZn-MOF/MoS <sub>2</sub> /PPy)	30	-49.18	1.5	15.88	4.56	1.5	/	Bi et al. <sup>73</sup>
FON (Fe/Fe <sub>3</sub> O <sub>4</sub> /FeN)/NC@PPy (Fe-MOF/PPy)	30	-60.08	1.44	/	5.1	1.64	12.9–18.0	Ma et al. <sup>54</sup>

composites are summarized in **Table 5**. The advantage of conductive polymers is their adjustable conductivity, which can optimize impedance matching; however, the optimization of absorption performance is not excellent compared with graphene and so on.

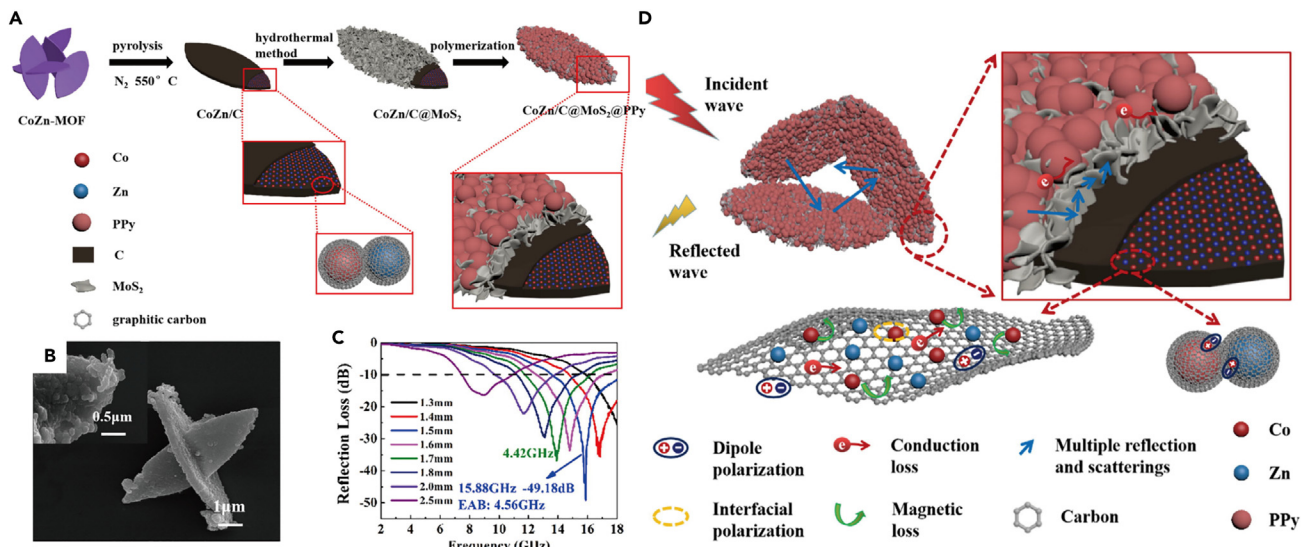
Bi et al. prepared CoZn/C@MoS<sub>2</sub>@PPy composites by MOF self-template method as shown in **Figure 8**<sup>73</sup> MoS<sub>2</sub> sheets and PPy shells were used to optimize impedance matching of 2D CoZn/C composites. CoZn/C@MoS<sub>2</sub>@PPy exhibited enhanced EMW absorption intensity compared to the directly carbonized MOF derivative of CoZn/C. When the thickness of CoZn/C@MoS<sub>2</sub>@PPy was 1.5 mm, the RL<sub>min</sub> reached -49.18 dB. The excellent EMW absorption performance was mainly attributed to the excellent dielectric loss, conduction loss, and optimized impedance matching of the CoZn/C@MoS<sub>2</sub>@PPy composite. Ma et al. synthesized a novel rod-like FON/NC (Fe/Fe<sub>3</sub>O<sub>4</sub>/FeN/N doped carbon) composite by a two-ligand strategy and subsequent calcination, then coated PPy on the FON/NC surface by simple polymerization.<sup>54</sup> The PPy layer effectively optimized impedance matching and significantly improved EMW absorption performance. The RL<sub>min</sub> reached -60.08 dB with a thickness of 1.44 mm, and the EAB was 5.06 GHz. The excellent EMW absorption properties benefited from a reasonable balance between the multi-component depletion mechanism and the unique microstructure. MOF-derived nanoporous Co/C-modified Co/C@ppy composites were prepared by self-assembly polymerization by Sun et al.<sup>171</sup> The RL<sub>min</sub> value reached -44.76 dB with a thickness of 2.5 mm, and the EAB was 6.56 GHz.

Conductive polymers are usually coated on the surface of the MOF derivative to enhance dielectric loss while adjusting impedance matching. However, as can be seen from **Table 5**, this composite method does not significantly optimize the absorption performance of MOF derivatives, both in terms of RL and EAB.

### MOF derivatives combined with magnetic nanoparticles (NPs) for EMW absorption

During carbonization, MOFs inevitably cause the reunion of magnetic particles in the carbon matrix, which forms large magnetic particles. In this case, the advantages of nano-level absorption will be limited. In addition, the formation of large-scale magnetic particles restricts magnetic response and reduces magnetic loss capacity. Taking advantage of the porous structure of MOFs to introduce additional magnetic particles or replace metals in MOFs is one of the most effective ways to enhance the magnetic properties of MOF derivatives. The EMW absorption performances of various magnetic NPs/MOF composites are summarized in **Table 6**. Magnetic NPs/MOFs have great advantages in the field of high-frequency absorption due to the enhanced magnetic effect.

Wang et al. prepared nanoporous Co/C composites by thermal carbonization process using Co NPs/ZIF-67 composites as raw materials as shown in **Figure 9**.<sup>172</sup> After carbonization at 700°C, the Co/C composites obtained the best EMW absorption properties. The RL<sub>min</sub> reached -30.31 dB at 3.0 mm, and the EAB reached 4.93 GHz with a thickness of 3.0 mm. Co NPs were embedded in the porous ZIF-67 matrix, which effectively reduced the complex dielectric constant of porous carbon, and optimized impedance matching, thereby improving the absorption performance. In addition, the porous Co NPs/graphite interface caused more interface polarization, which was conducive to the dielectric loss of EMW. Liu et al. synthesized Fe NPs (Fe/C) modified nanoporous carbons by mechanically mixing iron precursors (ferrous salts) with pre-synthesized ZIF 8 and then converting them to Fe NPs at high temperature.<sup>173</sup> After a high-temperature treatment of 1000°C, the Zn element evaporated, and the metal element in the carbon matrix was replaced by iron. The RL<sub>min</sub> reached -29.5 dB at 2.5 mm, and the EAB reached 3.0 GHz. The high porosity of graphitic

**Figure 8. The EMW absorption performance of CoZn/C@MoS<sub>2</sub>@PPy**(A) The schematic formation process of the CoZn/C@MoS<sub>2</sub>@PPy composites.(B) SEM images of the CoZn/C@MoS<sub>2</sub>@PPy.(C) The 2D reflection loss of CoZn/C@MoS<sub>2</sub>@PPy composites.(D) Schematic illustration of microwave absorption mechanism for CoZn/C@MoS<sub>2</sub>@Ppy. Reprinted and adapted with permission from ref.<sup>73</sup> Copyright 2021 Elsevier Inc.

carbon favors the uniform distribution of Fe NPs as well as the synergistic effect between Fe NPs and the carbon matrix. Zhang et al. synthesized a novel FeCo NP-embedded nanoporous carbon by *in situ* carbonization of dehydroascorbic acid (DHAA)-coated Fe<sub>3</sub>O<sub>4</sub> NPs encapsulated in ZIF 67.<sup>57</sup> The RL<sub>min</sub> reached -21.7 dB at 1.2 mm, and the EAB was 5.8 GHz. Wang et al. exploited the pore structure of the MOF and introduced additional Ni particles.<sup>174</sup> After carbonization at 800°C, the RL<sub>min</sub> reached -61.02 dB at 2.0 mm, and the EAB was 5.2 GHz.

The introduction of magnetic particles will make the minimum reflection absorption peak move to a higher frequency and achieve better absorption performance at relatively low thickness, but the oxidation problem of magnetic particles also limits its further practical application.

### MOF derivatives combined with other components for EMW absorption

Some transition metal oxides with excellent dielectric properties have the function of impedance adjustment. MnO<sub>2</sub> is an important transition metal oxide that has received extensive attention due to its advantages of low cost, diverse morphologies, and good thermal stability, and it can be used for impedance matching adjustment of EMW absorbing materials.<sup>175</sup> Wang et al. fabricated cubic hollow Co/N/C@MnO<sub>2</sub> composites for

**Table 6. EMW absorption performances of various magnetic NPs/MOF composites**

Composite (precursor)	Filling ratio (wt%)	Minimum RL			Maximum EAB			Reference
		Value (dB)	Thickness (mm)	f <sub>m</sub> (GHz)	Value (GHz)	Thickness (mm)	Range (GHz)	
Co/C (Co-MOF/Co NPs)	25	-30.31	3.0	11.3	4.93	3.0	8.3-13.2	Wang et al. <sup>172</sup>
Fe/C(Zn-MOF/Fe <sup>2+</sup> )	15	-29.50	2.5	17.2	4.30	3.0	13.7-18.0	Liu et al. <sup>173</sup>
FeCo/C (Co-MOF/Fe <sub>3</sub> O <sub>4</sub> )	50	-21.70	1.2	15.20	5.80	1.2	12.2-18.0	Zhang et al. <sup>57</sup>
CoNi/C (Co-MOF/NiCo-LDH)	10	-61.02	2.0	13.68	5.20	2.0	/	Wang et al. <sup>174</sup>
CoO/Co/C (Co-MOF/Co (OH) <sub>2</sub> )	70	-38.46	1.5	16.12	4.8	2.0	9.7-14.5	Wang et al. <sup>175</sup>
Co/NPC@Void@Cl (Co-MOF/Fe (CO) <sub>5</sub> )	40	-49.2	2.2	13.68	6.7	2.2	10.6-17.3	Quan et al. <sup>58</sup>

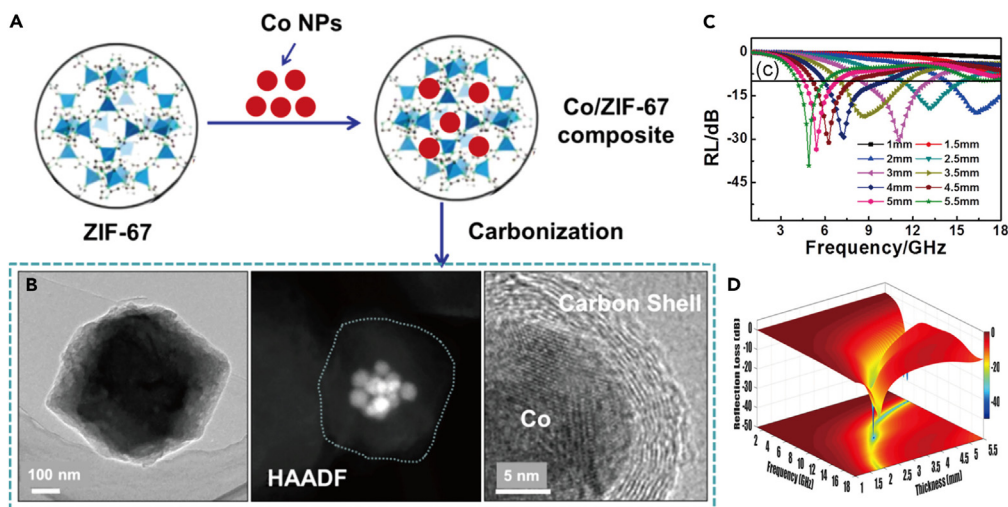


**Figure 9. The EMW absorption performance of Co NPs/ZIF-67**

(A) Synthetic route of Co NPs/ZIF-67 composites.

(B) TEM images of Co NPs/ZIF-67 composites.

(C) The 2D reflection loss of Co NPs/ZIF-67 composites.

(D) 3D maps of RL values for Co/C-700. Reprinted and adapted with permission from ref.<sup>172</sup> Copyright 2017, American Chemical Society.

EMW absorption via ZIF-67 self-templated strategy.<sup>177</sup> The introduction of MnO<sub>2</sub> improved the impedance mismatching caused by the excessively high dielectric constant. Improved impedance matching and coordination of various components were the main reasons for the excellent EMW absorption performance. The value of RL<sub>min</sub> was −58.9 dB.

Graphitic carbon nitride (g-C<sub>3</sub>N<sub>4</sub>) is a semiconductor material widely used in the field of photocatalysis.<sup>178–181</sup> Recently, due to its unique 2D structure and dielectric properties, it has gradually been applied to EMW absorbing materials.<sup>182–185</sup> Since g-C<sub>3</sub>N<sub>4</sub> is unstable at high temperatures, it decomposes almost completely into cyanide fragments at temperatures above 700°C, which can not only etch the carbon material to increase porosity but also dope additional nitrogen to create polarization sites, increasing the dielectric loss of EMW.<sup>186,187</sup> In addition, g-C<sub>3</sub>N<sub>4</sub> exhibits electronegativity due to the oxygen-containing functional groups on the surface, which provide conditions for the deposition of metal cations. Therefore, MOF/g-C<sub>3</sub>N<sub>4</sub> composites can be prepared by simple electrostatic self-assembly. Zhu et al. synthesized a series of MOF-Co@CNTs by annealing the ZIF-67/g-C<sub>3</sub>N<sub>4</sub> precursor.<sup>81</sup> The organic framework of ZIF was carbonized, and the cobalt ions in ZIF-67 were reduced to cobalt particles after heat treatment. Under the catalysis of Co, g-C<sub>3</sub>N<sub>4</sub> formed CNTs grown on the surface of ZIF-67 derivatives. CNTs can protect the Co particles encapsulated in them from corrosion while reducing the density of the material. In addition, the CNTs also formed a 3D network on the surface, which facilitated the absorption of EMW. After a carbonization temperature of 700°C, the RL<sub>min</sub> reached −59.5 dB at 1.6 mm, and the EAB was 5.27 GHz.

Silicon carbide (SiC) is an important wide-bandgap semiconductor material. SiC is used to prepare EMW absorbing materials due to its good thermal stability, high strength, light weight, and special electrical properties.<sup>188–191</sup> However, the defects of non-magnetic, single-polarization, and low conductivity limit the further optimization of its EMW absorbing properties. Combining magnetic MOF derivatives with SiC can not only introduce magnetic loss but also improve conductive loss by carbon derived from MOF. Yang et al. prepared multicomponent composites composed of SiC, Ni, NiO, and C NPs by annealing SiC NPs and Ni-MOFs in Ar.<sup>192</sup> The RL<sub>min</sub> of the SiC/Ni/NiO/C nanocomposite was improved compared to that of single SiC NPs and Ni-MOF, reaching −50.52 dB due to the rich interface created by the multicomponent and the improved conduction path of the introduced SiC NPs. However, the EAB was only 2.9 GHz. Compared with SiC NPs, SiC nanowires can be used as wires to connect MOF derivatives, to solve the problem of weak conductivity loss caused by the lack of continuous spatial structure between single MOF particles.<sup>145</sup> Zhang et al. connected MOFs in series through SiC nanowires by *in situ* growth to form a kebab structure composite.<sup>70</sup> The introduction of SiC nanowires built a spatially continuous phase

while increasing the MOF aspect ratio. Studies have shown that the composite achieved excellent EMW absorption performance whether it was calcined in an inert gas (Ar) atmosphere or an air atmosphere. The shrinking polyhedron remained in the air, but disintegrated into small particles under argon. The  $RL_{min}$  reached  $-47$  dB at 3 mm. In particular, the EAB was widened to 5.92 GHz with a thickness of 2 mm. The enhanced EMW absorption capability should be attributed to the combined effects of reduced dielectric constant, increased aspect ratio, and enhanced interfacial polarization.

Transition metal molybdenum-based materials, such as  $\text{MoO}_2$ ,  $\text{Mo}_2\text{C}$ ,  $\text{MoS}_2$ , and  $\text{Mo}_2\text{N}$ , are promising as EMW absorbers due to their low cost and chemical stability. Based on the excellent conductivity of  $\text{Mo}_2\text{N}$ , Xu et al. studied the EMW absorbers with  $\text{Mo}_2\text{N}$  composition for the first time.<sup>193</sup> First, core-shell  $\text{MoO}_3@\text{hollow-CoFe-PBA}$  was generated through *in situ* self-assembly and ligand exchange reactions of ZIF-67. Then, the final  $\text{Mo}_2\text{N}@\text{CoFe}@C/CNT$  composites were obtained by calcination in the presence of melamine. During the calcination process, CoFe NPs acted as a catalyst for graphitic carbon and melamine to catalyze the growth of CNTs on the surface of  $\text{Mo}_2\text{N}$  *in situ*, constructing a novel "tube-on-rod" structure. Dielectric  $\text{Mo}_2\text{N}$  acted as the core and magnetic CoFe NPs embedded in C/CNTs acted as the shell to construct a special core-shell structure. Based on the rich interface of core-shell structure, unique electron migration/hopping paths in graphitized C/CNT and  $\text{Mo}_2\text{N}$  rods and multi-scale magnetic coupling and enhanced magnetic responsiveness constructed by highly dispersed CoFe particles, the  $\text{Mo}_2\text{N}@\text{CoFe}@C/CNT$  exhibited excellent EMW absorption properties. The  $RL_{min}$  reached  $-53.5$  dB, and the EAB was 5.0 GHz.

## CONCLUSIONS AND PROSPECTS

The research progress of MOF derivative-based composites in the field of EMW absorption is reviewed in terms of compounding strategy. The MOF derivative-based composites are mainly divided into six categories: MOF combined with graphene, MOF combined with CNTs, MOF combined with BDC, MOF combined with MXene, MOF combined with a conductive polymer, and MOF combined with magnetic NPs. Abundant studies have shown that the EMW absorption performance has been effectively improved after the MOF derivatives are compounded with other materials. The introduction of graphene, CNTs, MXene, and BDC makes the independent MOF derivatives efficiently connected, which builds a sufficient conductive network to improve the loss capability. In addition, many heterointerfaces are generated in the recombination process, which leads to high interfacial polarization. However, the introduction of magnetic particles can enhance magnetic losses while adjusting the impedance matching of the dielectric material. Combined with the intrinsic loss capability of MOF derivatives as well as some special structures such as core-shell microstructure or hierarchically porous microstructure, the excellent EMW absorption performance of the MOF derivative-based composites can be accomplished.

Although some achievements have been made for MOF derivative-based composite in the field of EMW absorption, there are still many challenges and opportunities ahead. Firstly, the current research mainly focuses on the hybridization of materials, and the high-efficiency structural design of composites for improving EMW absorption performance remains rarely reported. Furthermore, the EMW absorption mechanism is generally expressed briefly as the synergy of various loss mechanisms in most reports, and more attention should be paid to the research of these mechanisms. Moreover, the research on environmental adaptability of the EMW absorbing materials for meeting complex application scenarios is still insufficient. Thus, in addition to the design of components, it is also necessary to introduce structural design to achieve the best absorption performance through the coordination of structure and components. In addition, combining with the guidance of theoretical simulation to design EMW absorption materials is also worth considering. Furthermore, to promote adaptability in multiple scenarios, some other functions such as heat insulation, thermal infrared stealth, and hydrophobicity should be considered.

To sum up, MOF derivative-based composites can efficiently improve the EMW absorption performance of MOF derivatives by optimizing the impedance matching and loss ability. However, a lot of challenges in MOF-based EMW absorbers still exist in practical applications, requiring increasing attention. We hope this review can guide the study of MOF derivative-based composites for achieving high-performance EMW absorption.

## LIMITATIONS OF THE STUDY

MOF derivatives are widely used for EMW absorbing materials due to their advantages of large specific surface area, controllable structure, and high porosity. However, the magnetic porous carbon obtained

by directly carbonizing the MOF suffers from poor impedance matching, a large filling amount, and a narrow EAB, which limits the practical application of such materials. Further research that focuses on compounding MOF derivatives with other types of materials to optimize MOF-based EMW absorbing performance is needed. However, more attention should be paid to the research of these compound mechanisms.

## ACKNOWLEDGMENTS

This work was supported by the National Key R&D Program of China (No. 2021YFB3502500), National Natural Science Foundation of China (NO. 22205131), Natural Science Foundation of Shandong Province (No. 2022HYQ-014, ZR2016BM16), and the New 20 Funded Programs for universities of Jinan (2021GXRC036), Provincial Key Research and Development Program of Shandong (2021ZLGX01), Natural Science Foundation of Jiangsu Province (NO.BK20222074), Shenzhen municipal special fund for guiding local scientific and Technological Development (China 2021Szvup071), the Joint Laboratory project of Electromagnetic Structure Technology (637-2022-70-F-037), and Qilu Young Scholar Program of Shandong University (No. 31370082163127).

## AUTHOR CONTRIBUTIONS

Conceptualization, J.L. and Z.Z.; Methodology, J.L., J.Q., Q.W., and Z.Z.; Investigation, J.L.; Writing – Original Draft, J.L.; Writing – Review and Editing, S.Z. and Z.Z.; Supervision, J.L. and Z.Z.; Funding Acquisition, J.L., W.L., and Z.Z.

## DECLARATION OF INTERESTS

There are no conflicts to declare.

## REFERENCES

1. Lv, H., Yang, Z., Liu, B., Wu, G., Lou, Z., Fei, B., and Wu, R. (2021). A flexible electromagnetic wave-electricity harvester. *Nat. Commun.* 12, 834.
2. Zhang, H., Xu, J., Wang, S., Liu, Q., and Kong, X. (2022). Constructing holey  $\gamma$ -Fe<sub>2</sub>O<sub>3</sub> nanosheets with enhanced capability for microwave absorption. *Mater. Today Chem.* 23, 100690.
3. Gao, S., Wang, G.-S., Guo, L., and Yu, S.-H. (2020). Tunable and Ultraefficient Microwave Absorption Properties of Trace N-Doped Two-Dimensional Carbon-Based Nanocomposites Loaded with Multi-Rare Earth Oxides. *Small* 16, 1906668.
4. Pan, F., Yu, L., Xiang, Z., Liu, Z., Deng, B., Cui, E., Shi, Z., Li, X., and Lu, W. (2021). Improved synergistic effect for achieving ultrathin microwave absorber of 1D Co nanochains/2D carbide MXene nanocomposite. *Carbon* 172, 506–515.
5. Zhao, J., Wei, Y., Zhang, Y., and Zhang, Q. (2022). 3D flower-like hollow CuS@PANI microspheres with superb X-band electromagnetic wave absorption. *J. Mater. Sci. Technol.* 126, 141–151.
6. Zhao, Z., Kou, K., Zhang, L., and Wu, H. (2022). Optimal particle distribution induced interfacial polarization in bouquet-like hierarchical composites for electromagnetic wave absorption. *Carbon* 186, 323–332.
7. Zhang, F., Yin, S., Chen, Y., Zheng, Q., Wang, L., and Jiang, W. (2022). Ligand-directed construction of CNTs-decorated metal carbide/carbon composites for ultra-strong and broad electromagnetic wave absorption. *Chem. Eng. J.* 433, 133586.
8. Gao, Z., Lan, D., Zhang, L., and Wu, H. (2021). Simultaneous Manipulation of Interfacial and Defects Polarization toward Zn/Co Phase and Ion Hybrids for Electromagnetic Wave Absorption. *Adv. Funct. Mater.* 31, 2106677.
9. Li, Q., Zhang, Z., Qi, L., Liao, Q., Kang, Z., and Zhang, Y. (2019). Toward the Application of High Frequency Electromagnetic Wave Absorption by Carbon Nanostructures. *Adv. Sci.* 6, 1801057.
10. Qin, M., Zhang, L., and Wu, H. (2022). Dielectric Loss Mechanism in Electromagnetic Wave Absorbing Materials. *Adv. Sci.* 9, 2105553. <https://doi.org/10.1002/advs.202105553>.
11. Lv, H., Yang, Z., Pan, H., and Wu, R. (2022). Electromagnetic absorption materials: Current progress and new frontiers. *Prog. Mater. Sci.* 127, 100946.
12. Jin, L., Yi, P., Wan, L., Hou, J., Chen, P., Zu, J., Wei, B., Yao, Z., and Zhou, J. (2022). Thickness-controllable synthesis of MOF-derived Ni@N-doped carbon hexagonal nanoflakes with dielectric-magnetic synergy toward wideband electromagnetic wave absorption. *Chem. Eng. J.* 427, 130940.
13. Quan, B., Shi, W., Ong, S.J.H., Lu, X., Wang, P.L., Ji, G., Guo, Y., Zheng, L., and Xu, Z.J. (2019). Defect Engineering in Two Common Types of Dielectric Materials for Electromagnetic Absorption Applications. *Adv. Funct. Mater.* 29, 1901236.
14. Wang, X., Lu, Y., Zhu, T., Chang, S., and Wang, W. (2020). CoFe<sub>2</sub>O<sub>4</sub>/N-doped reduced graphene oxide aerogels for high-performance microwave absorption. *Chem. Eng. J.* 388, 124317.
15. Li, J., Yang, S., Jiao, P., Peng, Q., Yin, W., Yuan, Y., Lu, H., He, X., and Li, Y. (2020). Three-dimensional macroassembly of hybrid C@CoFe nanoparticles/reduced graphene oxide nanosheets towards multifunctional foam. *Carbon* 157, 427–436.
16. Zhang, Y., Zhang, H.-B., Wu, X., Deng, Z., Zhou, E., and Yu, Z.-Z. (2019). Nanolayered Cobalt@Carbon Hybrids Derived from Metal–Organic Frameworks for Microwave Absorption. *ACS Appl. Nano Mater.* 2, 2325–2335.
17. Liu, Q., Cao, Q., Bi, H., Liang, C., Yuan, K., She, W., Yang, Y., and Che, R. (2016). CoNi@SiO<sub>2</sub>@TiO<sub>2</sub> and CoNi@Air@TiO<sub>2</sub> Microspheres with Strong Wideband Microwave Absorption. *Adv. Mater.* 28, 486–490.
18. Zeng, Q., Wang, L., Li, X., You, W., Zhang, J., Liu, X., Wang, M., and Che, R. (2021). Double ligand MOF-derived pomegranate-like Ni@C microspheres as high-performance microwave absorber. *Appl. Surf. Sci.* 538, 148051.
19. Xu, J., Zhang, X., Yuan, H., Zhang, S., Zhu, C., Zhang, X., and Chen, Y. (2020). N-doped reduced graphene oxide aerogels containing pod-like N-doped carbon nanotubes and FeNi nanoparticles for electromagnetic wave absorption. *Carbon* 159, 357–365.

20. Ma, J., Shu, J., Cao, W., Zhang, M., Wang, X., Yuan, J., and Cao, M. (2019). A green fabrication and variable temperature electromagnetic properties for thermal stable microwave absorption towards flower-like  $\text{Co}_3\text{O}_4@\text{rGO}/\text{SiO}_2$  composites. *Compos. B Eng.* 166, 187–195.
21. Zhao, H.-B., Cheng, J.-B., Zhu, J.-Y., and Wang, Y.-Z. (2019). Ultralight CoNi/rGO aerogels toward excellent microwave absorption at ultrathin thickness. *J. Mater. Chem. C* 7, 441–448.
22. Wei, Y., Lin, J., Jiang, T., Li, L., Zhong, K., Zhang, J., and Peng, Y. (2021). Optimization of microwave absorption properties of C/NiP microfiber composites. *Ceram. Int.* 47, 7937–7945.
23. Huang, B., Yue, J., Wei, Y., Huang, X., Tang, X., and Du, Z. (2019). Enhanced microwave absorption properties of carbon nanofibers functionalized by FeCo coatings. *Appl. Surf. Sci.* 483, 98–105.
24. Liu, C., Lin, Z., Chen, C., Kirk, D.W., and Xu, Y. (2019). Porous C/Ni composites derived from fluid coke for ultra-wide bandwidth electromagnetic wave absorption performance. *Chem. Eng. J.* 366, 415–422.
25. Li, C., Sui, J., Jiang, X., Zhang, Z., and Yu, L. (2020). Efficient broadband electromagnetic wave absorption of flower-like nickel/carbon composites in 2–40 GHz. *Chem. Eng. J.* 385, 123882.
26. Ye, W., Sun, Q., and Zhang, G. (2019). Effect of heat treatment conditions on properties of carbon-fiber-based electromagnetic-wave-absorbing composites. *Ceram. Int.* 45, 5093–5099.
27. Yang, Z., Zhang, Y., Li, M., Yang, L., Liu, J., Hou, Y., and Yang, Y. (2019). Surface Architecture of Ni-Based Metal Organic Framework Hollow Spheres for Adjustable Microwave Absorption. *ACS Appl. Nano Mater.* 2, 7888–7897.
28. Liu, Y., Zhou, X., Jia, Z., Wu, H., and Wu, G. (2022). Oxygen Vacancy-Induced Dielectric Polarization Prevails in the Electromagnetic Wave-Absorbing Mechanism for Mn-Based MOFs-Derived Composites. *Adv. Funct. Mater.* 32, 2204499.
29. Jia, Z., Zhang, X., Gu, Z., and Wu, G. (2022). MOF-derived Ni-Co bimetal/porous carbon composites as electromagnetic wave absorber. *Adv. Compos. Hybrid Mater.* 6, 28.
30. Liu, J., Liang, H., Wei, B., Yun, J., Zhang, L., and Wu, H. (2023). "Matryoshka Doll" Heterostructures Induce Electromagnetic Parameter Fluctuation to Tailor Electromagnetic Wave Absorption. *Small Struct.* 2200379.
31. Qiu, Y., Yang, H., Wen, B., Ma, L., and Lin, Y. (2021). Facile synthesis of nickel/carbon nanotubes hybrid derived from metal organic framework as a lightweight, strong and efficient microwave absorber. *J. Colloid Interface Sci.* 590, 561–570.
32. Yaghi, O.M., Li, G., and Li, H. (1995). Selective binding and removal of guests in a microporous metal-organic framework. *Nature* 378, 703–706.
33. Li, S., Gao, Y., Li, N., Ge, L., Bu, X., and Feng, P. (2021). Transition metal-based bimetallic MOFs and MOF-derived catalysts for electrochemical oxygen evolution reaction. *Energy Environ. Sci.* 14, 1897–1927.
34. Liu, J., Zhu, D., Guo, C., Vasileff, A., and Qiao, S.-Z. (2017). Design Strategies toward Advanced MOF-Derived Electrocatalysts for Energy-Conversion Reactions. *Adv. Energy Mater.* 7, 1700518.
35. Zhu, Y.-P., Yin, J., Abou-Hamad, E., Liu, X., Chen, W., Yao, T., Mohammed, O.F., and Alshareef, H.N. (2020). Highly Stable Phosphonate-Based MOFs with Engineered Bandgaps for Efficient Photocatalytic Hydrogen Production. *Adv. Mater.* 32, 1906368.
36. Du, R., Wu, Y., Yang, Y., Zhai, T., Zhou, T., Shang, Q., Zhu, L., Shang, C., and Guo, Z. (2021). Porosity Engineering of MOF-Based Materials for Electrochemical Energy Storage. *Adv. Energy Mater.* 11, 2100154.
37. Shrivastav, V., Sundriyal, S., Goel, P., Kaur, H., Tuteja, S.K., Vikrant, K., Kim, K.-H., Tiwari, U.K., and Deep, A. (2019). Metal-organic frameworks (MOFs) and their composites as electrodes for lithium battery applications: Novel means for alternative energy storage. *Coord. Chem. Rev.* 393, 48–78.
38. Liu, Y., Wu, H., Li, R., Wang, J., Kong, Y., Guo, Z., Jiang, H., Ren, Y., Pu, Y., Liang, X., et al. (2022). MOF-COF "Alloy" Membranes for Efficient Propylene/Propane Separation. *Adv. Mater.* 34, 2201423.
39. Qian, Q., Asinger, P.A., Lee, M.J., Han, G., Mirzahi Rodriguez, K., Lin, S., Benedetti, F.M., Wu, A.X., Chi, W.S., and Smith, Z.P. (2020). MOF-Based Membranes for Gas Separations. *Chem. Rev.* 120, 8161–8266.
40. Lü, Y., Wang, Y., Li, H., Lin, Y., Jiang, Z., Xie, Z., Kuang, Q., and Zheng, L. (2015). MOF-Derived Porous Co/C Nanocomposites with Excellent Electromagnetic Wave Absorption Properties. *ACS Appl. Mater. Interfaces* 7, 13604–13611.
41. Gao, S., Zhang, G., Wang, Y., Han, X., Huang, Y., and Liu, P. (2021). MOFs derived magnetic porous carbon microspheres constructed by core-shell Ni@C with high-performance microwave absorption. *J. Mater. Sci. Technol.* 88, 56–65.
42. Li, Z., Han, X., Ma, Y., Liu, D., Wang, Y., Xu, P., Li, C., and Du, Y. (2018). MOFs-Derived Hollow Co/C Microspheres with Enhanced Microwave Absorption Performance. *ACS Sustain. Chem. Eng.* 6, 8904–8913.
43. Liu, Y., Yao, Z., Zhou, J., Jin, L., Wei, B., and He, X. (2022). Facile synthesis of MOF-derived concave cube nanocomposite by self-templated toward lightweight and wideband microwave absorption. *Carbon* 186, 574–588.
44. Wu, Q., Wang, B., Fu, Y., Zhang, Z., Yan, P., and Liu, T. (2021). MOF-derived Co/CoO particles prepared by low temperature reduction for microwave absorption. *Chem. Eng. J.* 410, 128378.
45. Gao, Z., Iqbal, A., Hassan, T., Zhang, L., Wu, H., and Koo, C.M. (2022). Texture Regulation of Metal-Organic Frameworks, Microwave Absorption Mechanism-Oriented Structural Optimization and Design Perspectives. *Adv. Sci.* 9, 2204151.
46. Zhao, Z., Gao, Z., Lan, D., and Kou, K. (2021). MOFs-derived hollow materials for electromagnetic wave absorption: prospects and challenges. *J. Mater. Sci. Mater. Electron.* 32, 25631–25648.
47. Song, S., Tian, B., Zhang, M., Gao, X., Jie, L., Liu, P., and Li, J. (2021). A novel multi-cavity structured MOF derivative/porous graphene hybrid for high performance microwave absorption. *Carbon* 48, 279–287.
48. Huang, X., Wei, J., Zhang, Y., Qian, B., Jia, Q., Liu, J., Zhao, X., and Shao, G. (2022). Ultralight Magnetic and Dielectric Aerogels Achieved by Metal-Organic Framework Initiated Gelation of Graphene Oxide for Enhanced Microwave Absorption. *Nano-Micro Lett.* 14, 107.
49. Hu, Q., Yang, R., Yang, S., Huang, W., Zeng, Z., and Gui, X. (2022). Metal-Organic Framework-Derived Core–Shell Nanospheres Anchored on Fe-Filled Carbon Nanotube Sponge for Strong Wideband Microwave Absorption. *ACS Appl. Mater. Interfaces* 14, 10577–10587.
50. Li, X., Wang, L., Li, X., Zhang, J., Wang, M., and Che, R. (2021). Multi-dimensional  $\text{ZnO}@\text{MWCNTs}$  assembly derived from MOF heterojunction as highly efficient microwave absorber. *Carbon* 172, 15–25.
51. Chen, F., Zhang, S., Ma, B., Xiong, Y., Luo, H., Cheng, Y., Li, X., Wang, X., and Gong, R. (2022). Bimetallic CoFe-MOF@ $\text{Ti}_3\text{C}_2\text{T}_x$  MXene derived composites for broadband microwave absorption. *Chem. Eng. J.* 431, 134007.
52. Han, X., Huang, Y., Ding, L., Song, Y., Li, T., and Liu, P. (2021).  $\text{Ti}_3\text{C}_2\text{T}_x$  MXene Nanosheet/Metal-Organic Framework Composites for Microwave Absorption. *ACS Appl. Nano Mater.* 4, 691–701.
53. Wang, Y., Zhang, W., Wu, X., Luo, C., Wang, Q., Li, J., and Hu, L. (2017). Conducting polymer coated metal-organic framework nanoparticles: Facile synthesis and enhanced electromagnetic absorption properties. *Synth. Met.* 228, 18–24.
54. Ma, M., Bi, Y., Jiao, Z., Yue, J., Liao, Z., Wang, Y., Ma, Y., and Huang, W. (2022). Facile fabrication of metal-organic framework derived  $\text{Fe}/\text{Fe}_3\text{O}_4/\text{FeN}/\text{N-doped}$  carbon composites coated with PPY for superior microwave absorption. *J. Colloid Interface Sci.* 608, 525–535.
55. Zhao, H., Cheng, Y., Ma, J., Zhang, Y., Ji, G., and Du, Y. (2018). A sustainable route from biomass cotton to construct lightweight and

- high-performance microwave absorber. *Chem. Eng. J.* 339, 432–441.
56. Xiong, Y., Xu, L., Yang, C., Sun, Q., and Xu, X. (2020). Implanting FeCo/C nanocages with tunable electromagnetic parameters in anisotropic wood carbon aerogels for efficient microwave absorption. *J. Mater. Chem. A*, 8, 18863–18871.
  57. Zhang, X., Ji, G., Liu, W., Quan, B., Liang, X., Shang, C., Cheng, Y., and Du, Y. (2015). Thermal conversion of an  $\text{Fe}_3\text{O}_4$ @metal-organic framework: a new method for an efficient Fe-Co/nanoporous carbon microwave absorbing material. *Nanoscale* 7, 12932–12942.
  58. Quan, B., Liang, X., Ji, G., Ma, J., Ouyang, P., Gong, H., Xu, G., and Du, Y. (2017). Strong Electromagnetic Wave Response Derived from the Construction of Dielectric/Magnetic Media Heterostructure and Multiple Interfaces. *ACS Appl. Mater. Interfaces* 9, 9964–9974.
  59. Zhang, Z., Cai, Z., Wang, Z., Peng, Y., Xia, L., Ma, S., Yin, Z., and Huang, Y. (2021). A Review on Metal–Organic Framework-Derived Porous Carbon-Based Novel Microwave Absorption Materials. *Nano-Micro Lett.* 13, 56.
  60. Li, Q., Zhao, Y., Li, X., Wang, L., Li, X., Zhang, J., and Che, R. (2020). MOF Induces 2D GO to Assemble into 3D Accordion-Like Composites for Tunable and Optimized Microwave Absorption Performance. *Small* 16, 2003905.
  61. Xu, X., Ran, F., Fan, Z., Cheng, Z., Lv, T., Shao, L., and Liu, Y. (2020). Bimetallic Metal–Organic Framework-Derived Pomegranate-like Nanoclusters Coupled with CoNi-Doped Graphene for Strong Wideband Microwave Absorption. *ACS Appl. Mater. Interfaces* 12, 17870–17880.
  62. Ding, L., Huang, Y., Xu, Z., Yan, J., Liu, X., Li, T., and Liu, P. (2020). MIL-53(Fe) derived MCC/rGO nanoparticles with excellent broadband microwave absorption properties. *Compos. Commun.* 21, 100362.
  63. Yin, Y., Liu, X., Wei, X., Li, Y., Nie, X., Yu, R., and Shui, J. (2017). Magnetically Aligned Co-C/MWCNTs Composite Derived from MWNT-Interconnected Zeolitic Imidazolate Frameworks for a Lightweight and Highly Efficient Electromagnetic Wave Absorber. *ACS Appl. Mater. Interfaces* 9, 30850–30861.
  64. Jia, H., Xing, H., Ji, X., and Gao, S. (2019). Synergistic effect of hexagonal flake  $\text{Co}_3\text{O}_4$ @PANI core-shell composites with excellent microwave-absorbing properties. *J. Mater. Sci. Mater. Electron.* 30, 3386–3395.
  65. Zhang, X., Qiao, J., Jiang, Y., Wang, F., Tian, X., Wang, Z., Wu, L., Liu, W., and Liu, J. (2021). Carbon-Based MOF Derivatives: Emerging Efficient Electromagnetic Wave Absorption Agents. *Nano-Micro Lett.* 13, 135.
  66. Shu, R., Li, X., Tian, K., and Shi, J. (2022). Fabrication of bimetallic metal-organic frameworks derived  $\text{Fe}_3\text{O}_4$ /C decorated graphene composites as high-efficiency and broadband microwave absorbers. *Compos. B Eng.* 228, 109423.
  67. Wang, J., Wang, Q., Wang, W., Li, P., Zhao, Y., Zhai, J., Zhao, W., Zhang, H., Yun, J., Zhang, Z., et al. (2021). Hollow Ni/C microsphere@graphene foam with dual-spatial and porous structure on the microwave absorbing performance. *J. Alloys Compd.* 873, 159811.
  68. Deng, W., Li, T., Li, H., Dang, A., Liu, X., Zhai, J., and Wu, H. (2023). Morphology modulated defects engineering from MnO<sub>2</sub> supported on carbon foam toward excellent electromagnetic wave absorption. *Carbon* 206, 192–200.
  69. Guo, R., Zheng, Q., Wang, L., Fan, Y., and Jiang, W. (2022). Porous N-doped Ni/SiO<sub>2</sub>/graphene network: Three-dimensional hierarchical architecture for strong and broad electromagnetic wave absorption. *J. Mater. Sci. Technol.* 106, 108–117.
  70. Zhang, K., Wu, F., Xie, A., Sun, M., and Dong, W. (2017). In Situ Stringing of Metal Organic Frameworks by SiC Nanowires for High-Performance Electromagnetic Radiation Elimination. *ACS Appl. Mater. Interfaces* 9, 33041–33048.
  71. Zhou, J., Guo, F., Luo, J., Hao, G., Liu, G., Hu, Y., Zhang, G., Guo, H., Zhou, H., and Jiang, W. (2022). Designed 3D heterostructure with 0D/1D/2D hierarchy for low-frequency microwave absorption in the S-band. *J. Mater. Chem. C* 10, 1470–1478.
  72. Wang, H.-Y., Sun, X.-B., Yang, S.-H., Zhao, P.-Y., Zhang, X.-J., Wang, G.-S., and Huang, Y. (2021). 3D Ultralight Hollow NiCo Compound@MXene Composites for Tunable and High-Efficient Microwave Absorption. *Nano-Micro Lett.* 13, 206.
  73. Bi, Y., Ma, M., Liu, Y., Tong, Z., Wang, R., Chung, K.L., Ma, A., Wu, G., Ma, Y., He, C., et al. (2021). Microwave absorption enhancement of 2-dimensional CoZn/C@MoS<sub>2</sub>@PPy composites derived from metal-organic framework. *J. Colloid Interface Sci.* 600, 209–218.
  74. Deng, L., and Han, M. (2007). Microwave absorbing performances of multiwalled carbon nanotube composites with negative permeability. *Appl. Phys. Lett.* 91, 023119.
  75. Yuan, H., Wang, Y., Suo, B., Zhang, S., Dong, H., Yan, F., Zhu, C., and Chen, Y. (2021). Dielectric relaxation and magnetic resonance of nitrogen-doped graphene-coated FeNi nanoparticles on nitrogen-doped carbon nanosheets. *J. Alloys Compd.* 854, 157212.
  76. Quan, B., Liang, X., Ji, G., Cheng, Y., Liu, W., Ma, J., Zhang, Y., Li, D., and Xu, G. (2017). Dielectric polarization in electromagnetic wave absorption: Review and perspective. *J. Alloys Compd.* 728, 1065–1075.
  77. Li, M., Zhu, W., Li, X., Xu, H., Fan, X., Wu, H., Ye, F., Xue, J., Li, X., Cheng, L., and Zhang, L. (2022).  $\text{Ti}_3\text{C}_2\text{T}_{x}$ /MoS<sub>2</sub> Self-Rolling Rod-Based Foam Boosts Interfacial Polarization for Electromagnetic Wave Absorption. *Adv. Sci.* 9, 2201118.
  78. Yi, P., Yao, Z., Zhou, J., Wei, B., Lei, L., Tan, R., and Fan, H. (2021). Facile synthesis of 3D Ni@C nanocomposites derived from two kinds of petal-like Ni-based MOFs towards lightweight and efficient microwave absorbers. *Nanoscale* 13, 3119–3135.
  79. Cai, L., Pan, F., Zhu, X., Dong, Y., Shi, Y., Xiang, Z., Cheng, J., Jiang, H., Shi, Z., and Lu, W. (2022). Etching engineering and electrostatic self-assembly of N-doped MXene/hollow Co-ZIF hybrids for high-performance microwave absorbers. *Chem. Eng. J.* 434, 133865.
  80. Yang, M., Yuan, Y., Li, Y., Sun, X., Wang, S., Liang, L., Ning, Y., Li, J., Yin, W., Che, R., and Li, Y. (2020). Dramatically enhanced electromagnetic wave absorption of hierarchical CNT/Co/C fiber derived from cotton and metal-organic-framework. *Carbon* 161, 517–527.
  81. Zhu, X., Qiu, H., Chen, P., Chen, G., and Min, W. (2021). Graphitic carbon nitride ( $\text{g}-\text{C}_3\text{N}_4$ ) in situ polymerization to synthesize MOF-Co@CNTs as efficient electromagnetic microwave absorption materials. *Carbon* 176, 530–539.
  82. Song, G., Yang, K., Gai, L., Li, Y., An, Q., Xiao, Z., and Zhai, S. (2021). ZIF-67/CMC-derived 3D N-doped hierarchical porous carbon with in-situ encapsulated bimetallic sulfide and Ni NPs for synergistic microwave absorption. *Compos. Part A Appl. Sci. Manuf.* 149, 106584.
  83. Deng, B., Xiang, Z., Xiong, J., Liu, Z., Yu, L., and Lu, W. (2020). Sandwich-Like Fe& $\text{TiO}_2$ @C Nanocomposites Derived from MXene/Fe-MOFs Hybrids for Electromagnetic Absorption. *Nano-Micro Lett.* 12, 55.
  84. Wang, H.-Y., Sun, X.-B., and Wang, G.-S. (2021). A MXene-modulated 3D crosslinking network of hierarchical flower-like MOF derivatives towards ultra-efficient microwave absorption properties. *J. Mater. Chem. A* 9, 24571–24581.
  85. Shu, R., Li, W., Wu, Y., Zhang, J., and Zhang, G. (2019). Nitrogen-doped Co-C/MWCNTs nanocomposites derived from bimetallic metal-organic frameworks for electromagnetic wave absorption in the X-band. *Chem. Eng. J.* 362, 513–524.
  86. Shu, J.-C., Cao, W.-Q., and Cao, M.-S. (2021). Diverse Metal–Organic Framework Architectures for Electromagnetic Absorbers and Shielding. *Adv. Funct. Mater.* 31, 2100470.
  87. Xu, H., Yin, X., Zhu, M., Han, M., Hou, Z., Li, X., Zhang, L., and Cheng, L. (2017). Carbon Hollow Microspheres with a Designable Mesoporous Shell for High-Performance Electromagnetic Wave Absorption. *ACS Appl. Mater. Interfaces* 9, 6332–6341.
  88. Xu, H., Zhang, P., Li, R., Wu, W., Wang, S., Xu, Y., Li, X., Zhang, L., and Cheng, L. (2018). Mesoporous carbon hollow microspheres with red blood cell like morphology for

- efficient microwave absorption at elevated temperature. *Carbon* 21, 343–351.
89. Wu, G., Cheng, Y., Yang, Z., Jia, Z., Wu, H., Yang, L., Li, H., Guo, P., and Lv, H. (2018). Design of carbon sphere/magnetic quantum dots with tunable phase compositions and boost dielectric loss behavior. *Chem. Eng. J.* 333, 519–528.
90. Zhang, X., Wang, X., Meng, F., Chen, J., and Du, S. (2019). Broadband and strong electromagnetic wave absorption of epoxy composites filled with ultralow content of non-covalently modified reduced graphene oxides. *Carbon* 154, 115–124.
91. Kuang, B., Song, W., Ning, M., Li, J., Zhao, Z., Guo, D., Cao, M., and Jin, H. (2018). Chemical reduction dependent dielectric properties and dielectric loss mechanism of reduced graphene oxide. *Carbon* 127, 209–217.
92. Cao, M., Han, C., Wang, X., Zhang, M., Zhang, Y., Shu, J., Yang, H., Fang, X., and Yuan, J. (2018). Graphene nanohybrids: excellent electromagnetic properties for the absorbing and shielding of electromagnetic waves. *J. Mater. Chem. C* 6, 4586–4602.
93. Li, X., Guo, S., Li, W., Ren, X., Su, J., Song, Q., Sobrido, A.J., and Wei, B. (2019). Edge-rich MoS<sub>2</sub> grown on edge-oriented three-dimensional graphene glass for high-performance hydrogen evolution. *Nano Energy* 57, 388–397.
94. Cheng, J., Chen, S., Chen, D., Dong, L., Wang, J., Zhang, T., Jiao, T., Liu, B., Wang, H., Kai, J.-J., et al. (2018). Editable asymmetric all-solid-state supercapacitors based on high-strength, flexible, and programmable 2D-metal–organic framework/reduced graphene oxide self-assembled papers. *J. Mater. Chem. 6*, 20254–20266.
95. Cheng, J., Liang, J., Dong, L., Chai, J., Zhao, N., Ullah, S., Wang, H., Zhang, D., Imtiaz, S., Shan, G., and Zheng, G. (2018). Self-assembly of 2D-metal–organic framework/graphene oxide membranes as highly efficient adsorbents for the removal of Cs<sup>+</sup> from aqueous solutions. *RSC Adv.* 8, 40813–40822.
96. Cheng, J., Liu, K., Li, X., Huang, L., Liang, J., Zheng, G., and Shan, G. (2020). Nickel–metal–organic framework nanobelt based composite membranes for efficient Sr<sup>2+</sup> removal from aqueous solution. *Environ. Sci. Ecotechnol.* 3, 100035.
97. Xia, W., Qu, C., Liang, Z., Zhao, B., Dai, S., Qiu, B., Jiao, Y., Zhang, Q., Huang, X., Guo, W., et al. (2017). High-Performance Energy Storage and Conversion Materials Derived from a Single Metal–Organic Framework/Graphene Aerogel Composite. *Nano Lett.* 17, 2788–2795.
98. Xiao, P., Li, S., Yu, C., Wang, Y., and Xu, Y. (2020). Interface Engineering between the Metal–Organic Framework Nanocrystal and Graphene toward Ultrahigh Potassium-Ion Storage Performance. *ACS Nano* 14, 10210–10218.
99. Xu, X., Shi, W., Li, P., Ye, S., Ye, C., Ye, H., Lu, T., Zheng, A., Zhu, J., Xu, L., et al. (2017). Facile Fabrication of Three-Dimensional Graphene and Metal–Organic Framework Composites and Their Derivatives for Flexible All-Solid-State Supercapacitors. *Chem. Mater.* 29, 6058–6065.
100. Wang, C., Han, X., Xu, P., Zhang, X., Du, Y., Hu, S., Wang, J., and Wang, X. (2011). The electromagnetic property of chemically reduced graphene oxide and its application as microwave absorbing material. *Appl. Phys. Lett.* 98, 072906.
101. Zhang, K., Xie, A., Sun, M., Jiang, W., Wu, F., and Dong, W. (2017). Electromagnetic dissipation on the surface of metal organic framework (MOF)/reduced graphene oxide (RGO) hybrids. *Mater. Chem. Phys.* 199, 340–347.
102. Jinjiao, W., Jianfeng, Y., Jun, Y., and Hui, Z. (2020). Design of a novel carbon nanotube and metal–organic framework interpenetrated structure with enhanced microwave absorption properties. *Nanotechnology* 31, 394002.
103. Liu, L., Wang, L., Li, Q., Yu, X., Shi, X., Ding, J., You, W., Yang, L., Zhang, Y., and Che, R. (2019). High-Performance Microwave Absorption of MOF-Derived Core-Shell Co@N-doped Carbon Anchored on Reduced Graphene Oxide. *ChemNanoMat* 5, 558–565.
104. Wang, G., Lin, J., Shi, Y., Chang, X., Wang, Y., Guo, L., Wang, W., Dou, M., Deng, Y., Ming, R., and Zhang, J. (2019). Metal organic frameworks-derived Fe-Co nanoporous carbon/graphene composite as a high-performance electromagnetic wave absorber. *BMC Genom.* 20, 765–773.
105. Zhao, Y., Wang, W., Wang, J., Zhai, J., Lei, X., Zhao, W., Li, J., Yang, H., Tian, J., and Yan, J. (2021). Constructing multiple heterogeneous interfaces in the composite of bimetallic MOF-derivatives and rGO for excellent microwave absorption performance. *Carbon* 173, 1059–1072.
106. Liu, Z., Yuan, J., Li, K., Xiong, K., Jin, S., and Wang, P. (2018). Enhanced Electromagnetic Wave Absorption Performance of Co<sub>0.7</sub>Zn<sub>0.5</sub> ZIF-Derived Binary Co/ZnO and RGO Composites. *J. Electron. Mater.* 47, 4910–4918.
107. Wang, S., Xu, Y., Fu, R., Zhu, H., Jiao, Q., Feng, T., Feng, C., Shi, D., Li, H., and Zhao, Y. (2019). Rational Construction of Hierarchically Porous Fe-Co/N-Doped Carbon/GO Composites for Broadband Microwave Absorption. *Nano-Micro Lett.* 11, 76.
108. Wang, Y., He, D., and Wang, Y. (2021). Enhanced microwave absorption performance of MOF-derived hollow Zn-Co/C anchored on reduced graphene oxide. *Chin. Phys. B* 30, 067804.
109. Fan, X., Zhang, A., Li, M., Xu, H., Xue, J., Ye, F., and Cheng, L. (2020). A reduced graphene oxide/bi-MOF-derived carbon composite as high-performance microwave absorber with tunable dielectric properties. *J. Mater. Sci. Mater. Electron.* 31, 11774–11783.
110. Yu, W., Liu, B., and Zhao, X. (2022). Ultralight MOF-Derived Ni<sub>3</sub>S<sub>2</sub>@N, S-Codoped Graphene Aerogels for High-Performance Microwave Absorption. *Nanomaterials* 12, 655.
111. Zhang, K., Wu, F., Li, J., Sun, M., Xie, A., and Dong, W. (2018). Networks constructed by metal organic frameworks (MOFs) and multiwall carbon nanotubes (MCNTs) for excellent electromagnetic waves absorption. *Mater. Chem. Phys.* 208, 198–206.
112. Chen, C., Bao, S., Zhang, B., Chen, Y., Chen, W., and Wang, C. (2019). Coupling Fe@Fe<sub>3</sub>O<sub>4</sub> nanoparticles with multiple-walled carbon nanotubes with width band electromagnetic absorption performance. *Appl. Surf. Sci.* 467–468, 836–843.
113. Micheli, D., Apollo, C., Pastore, R., and Marchetti, M. (2010). X-Band microwave characterization of carbon-based nanocomposite material, absorption capability comparison and RAS design simulation. *Compos. Sci. Technol.* 70, 400–409.
114. Sianipar, M., Kim, S.H., Khairuddin, K., Iskandar, F., and Wenten, I.G. (2017). Functionalized carbon nanotube (CNT) membrane: progress and challenges. *RSC Adv.* 7, 51175–51198.
115. Ma, M., Zheng, Q., Zhang, X., Li, L., and Cao, M. (2023). VSe<sub>2</sub>/CNTs nanocomposites toward superior electromagnetic wave absorption performance. *Carbon* 212, 118159.
116. Liu, G., Wang, L., Zhang, H., Du, Z., Zhou, X., Wang, K., Sun, Y., and Gao, S. (2021). Cage-structured CoFe<sub>2</sub>O<sub>4</sub>@CNTs from Fe–Co-MOF confined growth in CNTs for high electromagnetic wave absorption performances. *Compos. Commun.* 27, 100910.
117. Wang, L., Huang, Y., Li, C., Chen, J., and Sun, X. (2015). Hierarchical graphene@Fe<sub>3</sub>O<sub>4</sub> nanocluster@carbon@MnO<sub>2</sub> nanosheet array composites: synthesis and microwave absorption performance. *Phys. Chem. Chem. Phys.* 17, 5878–5886.
118. Zhao, B., Li, Y., Ji, H., Bai, P., Wang, S., Fan, B., Guo, X., and Zhang, R. (2021). Lightweight graphene aerogels by decoration of 1D CoNi chains and CNTs to achieve ultra-wide microwave absorption. *Carbon* 176, 411–420.
119. Sabet, M., Jahangiri, H., and Ghashghaei, E. (2017). Improving microwave absorption of the polyaniline by carbon nanotube and needle-like magnetic nanostructures. *Synth. Met.* 224, 18–26.
120. Lu, S., Meng, Y., Wang, H., Wang, F., Yuan, J., Chen, H., Dai, Y., and Chen, J. (2019). Great enhancement of electromagnetic wave absorption of

- MWCNTs@carbonaceous CoO composites derived from MWCNTs-interconnected zeolitic imidazole framework. *Appl. Surf. Sci.* 481, 99–107.
121. Peibo, L., Yize, S., and Akinay, Y. (2020). The influence of MWCNTs on microwave absorption properties of Co/C and Ba-Hexaferrite hybrid nanocomposites. *Synth. Met.* 263, 116369.
122. Mirzaee, O., Huynen, I., and Zareinejad, M. (2021). Electromagnetic wave absorption characteristics of single and double layer absorbers based on trimetallic FeCoNi@C metal–organic framework incorporated with MWCNTs. *Synth. Met.* 271, 116634.
123. Fan, H., Yao, Z., Zhou, J., Yi, P., Wei, B., Lei, L., and Mao, Y. (2021). Enhanced microwave absorption of epoxy composite by constructing 3D Co–C–MWCNTs derived from metal organic frameworks. *J. Mater. Sci.* 56, 1426–1442.
124. Zhang, X., Cheng, J., Xiang, Z., Cai, L., and Lu, W. (2022). A hierarchical Co @ mesoporous C/macroporous C sheet composite derived from bimetallic MOF and oroxylum indicum for enhanced microwave absorption. *Carbon* 187, 477–487.
125. Wang, K., Zhang, S., Chu, W., Li, H., Chen, Y., Chen, B., Chen, B., and Liu, H. (2021). Tailoring conductive network nanostructures of ZIF-derived cobalt-decorated N-doped graphene/carbon nanotubes for microwave absorption applications. *J. Colloid Interface Sci.* 591, 463–473.
126. Pan, F., Liu, Z., Deng, B., Dong, Y., Zhu, X., Huang, C., Shi, Z., and Lu, W. (2021). Magnetic Fe<sub>3</sub>S<sub>4</sub> LTMCS micro-flowers@ wax gourd aerogel-derived carbon hybrids as efficient and sustainable electromagnetic absorber. *Carbon* 179, 554–565.
127. Pan, F., Liu, Z., Deng, B., Dong, Y., Zhu, X., Huang, C., and Lu, W. (2021). Lotus Leaf-Derived Gradient Hierarchical Porous C/MoS<sub>2</sub> Morphology Genetic Composites with Wideband and Tunable Electromagnetic Absorption Performance. *Nano-Micro Lett.* 13, 43.
128. Sun, X., Wang, Z., Wang, S., Ning, Y., Yang, M., Yang, S., Zhou, L., He, Q., and Li, Y. (2021). Ultrabroad-band and low-frequency microwave absorption based on activated waxberry metamaterial. *Chem. Eng. J.* 422, 130142.
129. Cheng, G., Pan, F., Zhu, X., Dong, Y., Cai, L., and Lu, W. (2021). Onion skin-derived hierarchical carbon/hollow CoFe<sub>2</sub>O<sub>4</sub> composite with effective microwave absorption in multi-band. *Compos. Commun.* 27, 100867.
130. Zhao, H., Cheng, Y., Zhang, Z., Zhang, B., Pei, C., Fan, F., and Ji, G. (2021). Biomass-derived graphene-like porous carbon nanosheets towards ultralight microwave absorption and excellent thermal infrared properties. *Carbon* 173, 501–511.
131. Xu, X., Ran, F., Lai, H., Cheng, Z., Lv, T., Shao, L., and Liu, Y. (2019). In Situ Confined Bimetallic Metal–Organic Framework Derived Nanostructure within 3D Interconnected Bamboo-like Carbon Nanotube Networks for Boosting Electromagnetic Wave Absorbing Performances. *ACS Appl. Mater. Interfaces* 11, 35999–36009.
132. Wang, J., Zhang, X., Li, Z., Ma, Y., and Ma, L. (2020). Recent progress of biomass-derived carbon materials for supercapacitors. *J. Power Sources* 451, 227794.
133. He, M., Sun, Y., and Han, B. (2013). Green Carbon Science: Scientific Basis for Integrating Carbon Resource Processing, Utilization, and Recycling. *Angew. Chem. Int. Ed.* 52, 9620–9633.
134. Bi, Z., Kong, Q., Cao, Y., Sun, G., Su, F., Wei, X., Li, X., Ahmad, A., Xie, L., and Chen, C.-M. (2019). Biomass-derived porous carbon materials with different dimensions for supercapacitor electrodes: a review. *J. Mater. Chem. B*, 16028–16045.
135. Dong, S., Tang, W., Hu, P., Zhao, X., Zhang, X., Han, J., and Hu, P. (2019). Achieving Excellent Electromagnetic Wave Absorption Capabilities by Construction of MnO Nanorods on Porous Carbon Composites Derived from Natural Wood via a Simple Route. *ACS Sustain. Chem. Eng.* 7, 11795–11805.
136. Li, X., Cui, E., Xiang, Z., Yu, L., Xiong, J., Pan, F., and Lu, W. (2020). Fe@NPC@CF nanocomposites derived from Fe-MOFs/ biomass cotton for lightweight and high-performance electromagnetic wave absorption applications. *J. Alloys Compd.* 819, 152952.
137. Xi, J., Zhou, E., Liu, Y., Gao, W., Ying, J., Chen, Z., and Gao, C. (2017). Wood-based straightway channel structure for high performance microwave absorption. *Carbon* 124, 492–498.
138. Wu, F., Liu, Z., Xiu, T., Zhu, B., Khan, I., Liu, P., Zhang, Q., and Zhang, B. (2021). Fabrication of ultralight helical porous carbon fibers with CNTs-confined Ni nanparticles for enhanced microwave absorption. *Compos. B Eng.* 215, 108814.
139. Wu, Z., Tian, K., Huang, T., Hu, W., Xie, F., Wang, J., Su, M., and Li, L. (2018). Hierarchically Porous Carbons Derived from Biomasses with Excellent Microwave Absorption Performance. *ACS Appl. Mater. Interfaces* 10, 11108–11115.
140. Qiu, X., Wang, L., Zhu, H., Guan, Y., and Zhang, Q. (2017). Lightweight and efficient microwave absorbing materials based on walnut shell-derived nano-porous carbon. *Nanoscale* 9, 7408–7418.
141. Wang, H., Meng, F., Li, J., Li, T., Chen, Z., Luo, H., and Zhou, Z. (2018). Carbonized Design of Hierarchical Porous Carbon/ Fe<sub>3</sub>O<sub>4</sub>@Fe Derived from Loofah Sponge to Achieve Tunable High-Performance Microwave Absorption. *ACS Sustain. Chem. Eng.* 6, 11801–11810.
142. Zhao, H., Cheng, Y., Lv, H., Ji, G., and Du, Y. (2019). A novel hierarchically porous magnetic carbon derived from biomass for strong lightweight microwave absorption. *Carbon* 142, 245–253.
143. Huang, L., Li, J., Wang, Z., Li, Y., He, X., and Yuan, Y. (2019). Microwave absorption enhancement of porous C@CoFe<sub>2</sub>O<sub>4</sub> nanocomposites derived from eggshell membrane. *Carbon* 143, 507–516.
144. Sun, X., Yang, M., Yang, S., Wang, S., Yin, W., Che, R., and Li, Y. (2019). Ultrabroad Band Microwave Absorption of Carbonized Waxberry with Hierarchical Structure. *Small* 15, 1902974.
145. Zhou, Y., Zhou, W., Ni, C., Yan, S., Yu, L., and Li, X. (2022). “Tree blossom” Ni/NC/C composites as high-efficiency microwave absorbents. *Chem. Eng. J.* 430, 132621.
146. Di, X., Wang, Y., Lu, Z., Cheng, R., Yang, L., and Wu, X. (2021). Heterostructure design of Ni/porous carbon nanosheet composite for enhancing the electromagnetic wave absorption. *Carbon* 179, 566–578.
147. Wu, Z., Yang, Z., Jin, C., Zhao, Y., and Che, R. (2021). Accurately Engineering 2D/2D/0D Heterojunction In Hierarchical Ti<sub>3</sub>C<sub>2</sub>T<sub>x</sub> MXene Nanoarchitectures for Electromagnetic Wave Absorption and Shielding. *ACS Appl. Mater. Interfaces* 13, 5866–5876.
148. Fu, J., Li, L., Yun, J.M., Lee, D., Ryu, B.K., and Kim, K.H. (2019). Two-dimensional titanium carbide (MXene)-wrapped sisal-Like NiCo<sub>2</sub>S<sub>4</sub> as positive electrode for High-performance hybrid pouch-type asymmetric supercapacitor. *Chem. Eng. J.* 375, 121939.
149. Lukatskaya, M.R., Mashtalir, O., Ren, C.E., Dall’Agnese, Y., Rozier, P., Taberna, P.L., Naguib, M., Simon, P., Barsoum, M.W., and Gogotsi, Y. (2013). Cation Intercalation and High Volumetric Capacitance of Two-Dimensional Titanium Carbide. *Science* 341, 1502–1505.
150. Hu, M., Zhang, H., Hu, T., Fan, B., Wang, X., and Li, Z. (2020). Emerging 2D MXenes for supercapacitors: status, challenges and prospects. *Chem. Soc. Rev.* 49, 6666–6693.
151. Han, X., Huang, Y., Gao, S., Zhang, G., Li, T., and Liu, P. (2021). A hierarchical carbon Fiber@MXene@ZnO core-sheath synergistic microstructure for efficient microwave absorption and photothermal conversion. *Carbon* 183, 872–883.
152. Cao, M.-S., Cai, Y.-Z., He, P., Shu, J.-C., Cao, W.-Q., and Yuan, J. (2019). 2D MXenes: Electromagnetic property for microwave absorption and electromagnetic interference shielding. *Chem. Eng. J.* 359, 1265–1302.
153. Naguib, M., Mochalin, V.N., Barsoum, M.W., and Gogotsi, Y. (2014). 25th Anniversary Article: MXenes: A New Family of Two-Dimensional Materials. *Adv. Mater.* 26, 992–1005.

154. Wang, B., Li, S., Huang, F., Wang, S., Zhang, H., Liu, F., and Liu, Q. (2022). Construction of multiple electron transfer paths in 1D core-shell heterostructures with MXene as interlayer enabling efficient microwave absorption. *Carbon* 187, 56–66.
155. Song, Q., Ye, F., Kong, L., Shen, Q., Han, L., Feng, L., Yu, G., Pan, Y., and Li, H. (2020). Graphene and MXene Nanomaterials: Toward High-Performance Electromagnetic Wave Absorption in Gigahertz Band Range. *Adv. Funct. Mater.* 30, 2000475.
156. Liao, Q., He, M., Zhou, Y., Nie, S., Wang, Y., Wang, B., Yang, X., Bu, X., and Wang, R. (2018). Rational Construction of  $Ti_3C_2T_x/Co$ -MOF-Derived Laminated Co/TiO<sub>2</sub>-C Hybrids for Enhanced Electromagnetic Wave Absorption. *Langmuir* 34, 15854–15863.
157. Wu, F., Liu, Z., Wang, J., Shah, T., Liu, P., Zhang, Q., and Zhang, B. (2021). Template-free self-assembly of MXene and CoNi-bimetal MOF into intertwined one-dimensional heterostructure and its microwave absorbing properties. *Chem. Eng. J.* 422, 130591.
158. Chang, M., Li, Q., Jia, Z., Zhao, W., and Wu, G. (2023). Tuning microwave absorption properties of Ti3C2Tx MXene-based materials: Component optimization and structure modulation. *J. Mater. Sci. Technol.* 148, 150–170.
159. Zhang, S., Jia, Z., Zhang, Y., and Wu, G. (2023). Electrospun Fe0.64Ni0.36/MXene/CNFs nanofibrous membranes with multicomponent heterostructures as flexible electromagnetic wave absorbers. *Nano Res.* 16, 3395–3407.
160. Miao, P., Cao, J., Kong, J., Li, J., Wang, T., and Chen, K.-J. (2020). Bimetallic MOF-derived hollow ZnNiC nano-boxes for efficient microwave absorption. *Nanoscale* 12, 13311–13315.
161. Zhou, C., Geng, S., Xu, X., Wang, T., Zhang, L., Tian, X., Yang, F., Yang, H., and Li, Y. (2016). Lightweight hollow carbon nanospheres with tunable sizes towards enhancement in microwave absorption. *Carbon* 108, 234–241.
162. Yan, F., Guo, D., Zhang, S., Li, C., Zhu, C., Zhang, X., and Chen, Y. (2018). An ultra-small NiFe<sub>2</sub>O<sub>4</sub> hollow particle/graphene hybrid: fabrication and electromagnetic wave absorption property. *Nanoscale* 10, 2697–2703.
163. Yan, J., Huang, Y., Liu, X., Zhao, X., Li, T., Zhao, Y., and Liu, P. (2021). Polypyrrole-Based Composite Materials for Electromagnetic Wave Absorption. *Polym. Rev.* 61, 646–687.
164. Liu, P., Huang, Y., Yang, Y., Yan, J., and Zhang, X. (2016). Sandwich structures of graphene@Fe<sub>3</sub>O<sub>4</sub>@PANI decorated with TiO<sub>2</sub> nanosheets for enhanced electromagnetic wave absorption properties. *J. Alloys Compd.* 662, 63–68.
165. Zhang, B., Du, Y., Zhang, P., Zhao, H., Kang, L., Han, X., and Xu, P. (2013). Microwave absorption enhancement of Fe<sub>3</sub>O<sub>4</sub>/polyaniline core/shell hybrid microspheres with controlled shell thickness. *J. Appl. Polym. Sci.* 130, 1909–1916.
166. Hosseini, S.H., Mohseni, S.H., Asadnia, A., and Kerdari, H. (2011). Synthesis and microwave absorbing properties of polyaniline/MnFe<sub>2</sub>O<sub>4</sub> nanocomposite. *J. Alloys Compd.* 509, 4682–4687.
167. Ding, J., Wang, L., Zhao, Y., Xing, L., Yu, X., Chen, G., Zhang, J., and Che, R. (2019). Boosted Interfacial Polarization from Multishell TiO<sub>2</sub>@Fe<sub>3</sub>O<sub>4</sub>@PPy Heterojunction for Enhanced Microwave Absorption. *Small* 15, 1902885.
168. Gai, L., Zhao, Y., Song, G., An, Q., Xiao, Z., Zhai, S., and Li, Z. (2020). Construction of core-shell PPy@MoS<sub>2</sub> with nanotube-like heterostructures for electromagnetic wave absorption: Assembly and enhanced mechanism. *Compos. Part A Appl. Sci. Manuf.* 136, 105965.
169. Zhang, M., Jin, X., Sun, R., Xiong, X., Wang, J., Xie, D., and Zhao, M. (2021). Hollow microspheres of polypyrrole/magnetite/carbon nanotubes by spray-dry as an electromagnetic synergistic microwave absorber. *Carbon* 19, 499–508.
170. Ma, Y., Ma, M., Yin, X., Shao, Q., Lu, N., Feng, Y., Lu, Y., Wujcik, E.K., Mai, X., Wang, C., and Guo, Z. (2018). Tuning polyaniline nanostructures via end group substitutions and their morphology dependent electrochemical performances. *Polymer* 156, 128–135.
171. Sun, X., Lv, X., Sui, M., Weng, X., Li, X., and Wang, J. (2018). Decorating MOF-Derived Nanoporous Co/C in Chain-Like Polypyrrole (PPy) Aerogel: A Lightweight Material with Excellent Electromagnetic Absorption. *Materials* 11, 781.
172. Wang, H., Xiang, L., Wei, W., An, J., He, J., Gong, C., and Hou, Y. (2017). Efficient and Lightweight Electromagnetic Wave Absorber Derived from Metal Organic Framework-Encapsulated Cobalt Nanoparticles. *ACS Appl. Mater. Interfaces* 9, 42102–42110.
173. Liu, Q., Liu, X., Feng, H., Shui, H., and Yu, R. (2017). Metal organic framework-derived Fe/carbon porous composite with low Fe content for lightweight and highly efficient electromagnetic wave absorber. *Chem. Eng. J.* 314, 320–327.
174. Wang, Y.-L., Yang, S.-H., Wang, H.-Y., Wang, G.-S., Sun, X.-B., and Yin, P.-G. (2020). Hollow porous CoNi/C composite nanomaterials derived from MOFs for efficient and lightweight electromagnetic wave absorber. *Carbon* 167, 485–494.
175. Wang, X., Zhou, P., Qiu, G., Zhang, X., Wang, L., Zhang, Q., Wang, M., and Liu, Z. (2020). Excellent electromagnetic wave absorption properties of porous core-shell CoO/Co/C nanocomposites derived from a needle-shaped Co(OH)<sub>2</sub>@ZIF-67 template. *J. Alloys Compd.* 842, 155807.
176. Shao, Y., Lu, W., Chen, H., Xiao, J.Q., Qiu, Y., and Chou, T.-W. (2018). Flexible ultra-thin Fe<sub>3</sub>O<sub>4</sub>/MnO<sub>2</sub> core-shell decorated CNT composite with enhanced electromagnetic wave absorption performance. *Compos. B Eng.* 144, 111–117.
177. Wang, R., He, M., Zhou, Y., Nie, S., Wang, Y., Liu, W., He, Q., Wu, W., Bu, X., and Yang, X. (2020). Metal-organic frameworks self-templated cubic hollow Co/N/C@MnO<sub>2</sub> composites for electromagnetic wave absorption. *Carbon* 156, 378–388.
178. Zhang, W., Zhang, Z., Kwon, S., Zhang, F., Stephen, B., Kim, K.K., Jung, R., Kwon, S., Chung, K.-B., and Yang, W. (2017). Photocatalytic improvement of Mn-adsorbed g-C<sub>3</sub>N<sub>4</sub>. *Appl. Catal. B* 206, 271–281.
179. Xu, T., Xia, Z., Li, H., Niu, P., Wang, S., and Li, L. Constructing Crystalline g-C<sub>3</sub>N<sub>4</sub>/g-C<sub>3</sub>N<sub>4-x</sub>S<sub>x</sub> Isotype Heterostructure for Efficient Photocatalytic and Piezocatalytic Performances. *ENERGY ENVIRON. MATER.* 0, 1–9.
180. Jiang, Z., Zhang, X., Chen, H.-S., Yang, P., and Jiang, S.P. (2020). Fusiform-Shaped g-C<sub>3</sub>N<sub>4</sub> Capsules with Superior Photocatalytic Activity. *Small* 16, 2003910.
181. She, X., Wu, J., Xu, H., Zhong, J., Wang, Y., Song, Y., Nie, K., Liu, Y., Yang, Y., Rodrigues, M.-T.F., et al. (2017). High Efficiency Photocatalytic Water Splitting Using 2D  $\alpha$ -Fe<sub>2</sub>O<sub>3</sub>/g-C<sub>3</sub>N<sub>4</sub> Z-Scheme Catalysts. *Adv. Energy Mater.* 7, 1700025.
182. Peymanfar, R., Selseleh-Zakerin, E., and Ahmadi, A. (2021). Tailoring energy band gap and microwave absorbing features of graphite-like carbon nitride (g-C<sub>3</sub>N<sub>4</sub>). *J. Alloys Compd.* 867, 159039.
183. Lv, H., Zhou, X., Wu, G., Kara, U.I., and Wang, X. (2021). Engineering defects in 2D g-C<sub>3</sub>N<sub>4</sub> for wideband, efficient electromagnetic absorption at elevated temperature. *J. Mater. Chem. B* 9, 19710–19718.
184. Lv, H., Zhang, H., and Ji, G. (2016). Development of Novel Graphene/g-C<sub>3</sub>N<sub>4</sub> Composite with Broad-Frequency and Light-Weight Features. *Part. Part. Syst. Char.* 33, 656–663.
185. Green, M., Liu, Z., Smedley, R., Nawaz, H., Li, X., Huang, F., and Chen, X. (2018). Graphitic carbon nitride nanosheets for microwave absorption. *Mater. Today Phys.* 5, 78–86.
186. Jin, H., Wang, J., Yang, S., Wu, Q., and Zhang, B. (2021). ZIF-67-derived micron-sized cobalt-doped porous carbon-based microwave absorbers with g-C<sub>3</sub>N<sub>4</sub> as template. *Ceram. Int.* 47, 11506–11513.
187. Ren, S., Yu, H., Wang, L., Huang, Z., Lin, T., Huang, Y., Yang, J., Hong, Y., and Liu, J. (2022). State of the Art and Prospects in Metal-Organic Framework-Derived

- Microwave Absorption Materials. *Nano-Micro Lett.* 14, 68.
188. Han, M., Yin, X., Hou, Z., Song, C., Li, X., Zhang, L., and Cheng, L. (2017). Flexible and Thermostable Graphene/SiC Nanowire Foam Composites with Tunable Electromagnetic Wave Absorption Properties. *ACS Appl. Mater. Interfaces* 9, 11803–11810.
189. Bechelany, M., Brioude, A., Stadelmann, P., Ferro, G., Cornu, D., and Miele, P. (2007). Very Long SiC-Based Coaxial Nanocables with Tunable Chemical Composition. *Adv. Funct. Mater.* 17, 3251–3257.
190. Mélinon, P., Masenelli, B., Tournus, F., and Perez, A. (2007). Playing with carbon and silicon at the nanoscale. *Nat. Mater.* 6, 479–490.
191. Wu, R., Zhou, K., Yue, C.Y., Wei, J., and Pan, Y. (2015). Recent progress in synthesis, properties and potential applications of SiC nanomaterials. *Prog. Mater. Sci.* 72, 1–60.
192. Yang, R., Yuan, J., Yu, C., Yan, K., Fu, Y., Xie, H., Chen, J., Chu, P.K., and Wu, X. (2020). Efficient electromagnetic wave absorption by SiC/Ni/NiO/C nanocomposites. *J. Alloys Compd.* 816, 152519.
193. Xu, C., Wang, L., Li, X., Qian, X., Wu, Z., You, W., Pei, K., Qin, G., Zeng, Q., Yang, Z., et al. (2021). Hierarchical Magnetic Network Constructed by CoFe Nanoparticles Suspended Within "Tubes on Rods" Matrix Toward Enhanced Microwave Absorption. *Nano-Micro Lett.* 13, 47.